



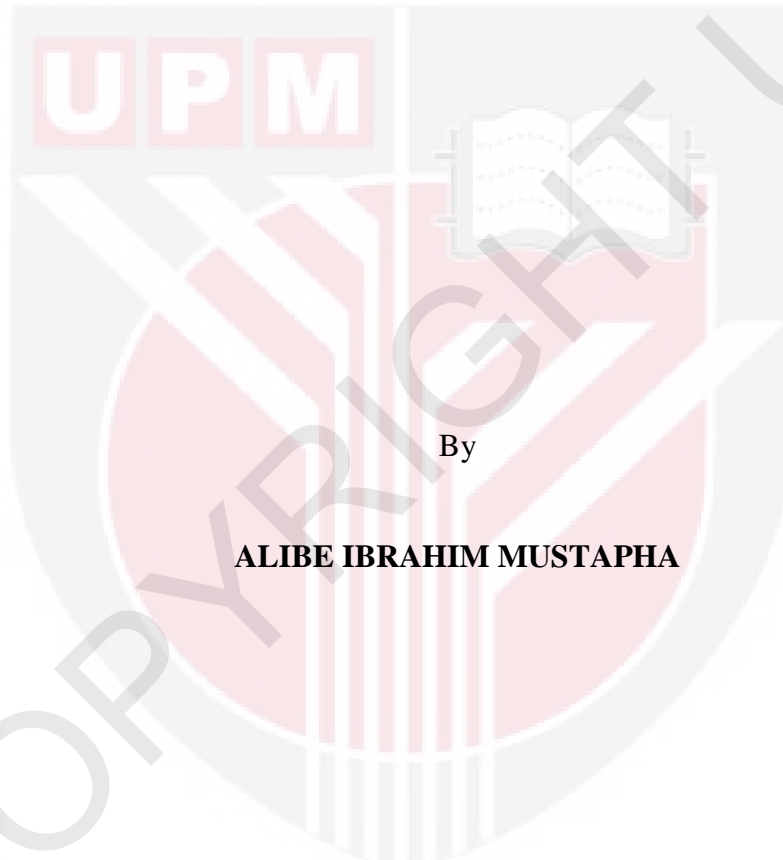
***STRUCTURAL AND OPTICAL PROPERTIES OF WILLEMITE
NANOPARTICLES SYNTHESIZED BY POLYMER THERMAL
TREATMENT METHOD***

ALIBE IBRAHIM MUSTAPHA

ITMA 2019 2



**STRUCTURAL AND OPTICAL PROPERTIES OF WILLEMITE
NANOPARTICLES SYNTHESIZED BY POLYMER THERMAL
TREATMENT METHOD**



**Thesis Submitted to the School of Graduate Studies, Universiti Putra Malaysia,
in Fulfillment of the Requirements for the Degree of Doctor of Philosophy**

February 2019

COPYRIGHT

All materials contained within the thesis, including without limitation text, logos, icons, photograph and all other artwork, is a copyright material of the Universiti Putra Malaysia unless otherwise stated. Use may be made of any material contained in the thesis for non-commercial purposes from the copyright holder. Commercial use of material may only be made with the express, prior written permission of Universiti Putra Malaysia.

Copyright © Universiti Putra Malaysia



DEDICATION

This thesis solely dedicated to my beloved parent, Hon. Mustapha Ali Benishiekh
and Zara Kellu Alibe.



Abstract of a thesis presented to the Senate of Universiti Putra Malaysia in fulfillment of the requirements for the degree Doctor of Philosophy.

STRUCTURAL AND OPTICAL PROPERTIES OF WILLEMITE NANOPARTICLES SYNTHESIZED BY POLYMER THERMAL TREATMENT METHOD

By

ALIBE IBRAHIM MUSTAPHA

February 2019

**Chairman : Khamirul Amin Matori, PhD
Institute : Advanced Technology**

Willemite is an inorganic phosphor material used for optoelectronic applications. Much attention has been paid to the synthesis of willemite nanoparticles in the last two decades. This includes the application of new methods or modification of the existing ones. The present study proposes a polymer thermal treatment method involving calcination temperature between 500 to 1000 °C to fabricate the willemite nanoparticles. The effects of synthesis parameters such as the calcination temperature, calcination holding time, PVP concentration, and the precursor concentration were extensively studied and optimized. The FT-IR, Raman and the XRD analysis revealed that the samples were amorphous at room temperature and further confirmed the formation of pure willemite nanoparticles upon the calcination process. The crystallite size of the materials ranges between 21.60–32.15 nm and increases with the increment of the calcination temperatures, calcination holding time and precursor. While the crystallite size was found to be reduced from 36.70–23.80 nm with the increase in the PVP concentration (2–5 g) for the willemite nanoparticles produced at 900 °C. This is in a good agreement with the particle size determined by HR-TEM and FESEM micrographs. The E_{opt} values decreased with the increased of holding times over the range of 5.39 eV at 1 h to 5.27 at 4 h. The E_{opt} of the material was also found to be increasing from 5.24–5.32 eV with the corresponding increase in the PVP concentration. The PL emission spectra reveal a blue emission at 485 nm due to zinc interstitial. For all the synthesis condition, the PL emission was found to be depended on the particle size of the willemite. The current findings provide a pathway to reduce the high energy consumed in the synthesis of willemite nanoparticles, and the wide band gap energy of the material may have key potential applications for future optoelectronic lighting devices.

Abstrak tesis yang dikemukakan kepada Senat Universiti Putra Malaysia sebagai memenuhi keperluan untuk ijazah Doktor Falsafah

CIRI-CIRI STRUKTUR DAN OPTIK NANOPARTIKEL WILLEMITE YANG DISINTESIS DENGAN KAEDAH RAWATAN HABA POLIMER

Oleh

ALIBE IBRAHIM MUSTAPHA

Februari 2019

Pengerusi : Khamirul Amin B Matori, PhD
Institut : Teknologi Maju

Willemite adalah bahan fosfor tidak organik yang digunakan untuk aplikasi optoelektronik. Terdapat banyak perhatian telah diberikan terhadap penghasilan nanopartikel willemite sejak dua dekad yang lalu. Ini termasuk penerapan kaedah baru atau pengubahsuaian yang sedia ada. Penyelidikan ini bertujuan untuk menghasilkan nanopartikel willemite yang melibatkan suhu kalsinasi antara 500 hingga 1000 °C menggunakan kaedah rawatan termal polimer baru. Kesan parameter seperti suhu kalsinasi, masa pemangkinan kalsin, kepekatan PVP dan kepekatan prekursor telah dikaji dan dioptimumkan secara meluas. FT-IR, Raman dan analisis XRD menunjukkan bahawa sampel adalah amorfus pada suhu bilik dan selanjutnya mengesahkan pembentukan nanopartikel willemite tulen apabila proses pengkalsinan dijalankan. Saiz kristal bahan adalah antara 21.60–32.15 nm dan bertambah dengan peningkatan suhu kalsinasi, masa pemangkinan kalsinasi dan prekursor. Walaupun saiz kristal didapati berkurang dari 36.7–23.8 nm dengan peningkatan kepekatan PVP (2–5 g) untuk nanopartikel willemite terhasil pada suhu 900 °C. Hasil ini bersesuaian dan bertepatan dengan saiz zarah yang ditentukan oleh HR-TEM dan mikrograf FESEM. Nilai E_{opt} yang diperolehi berkurangan dengan peningkatan tempoh masa iaitu antara 5.39 eV pada 1 jam ke 5.27 eV pada 4 jam. Tenaga jurang jalur optik bahan didapati meningkat daripada 5.24–5.32 eV dengan peningkatan yang sama dalam kepekatan PVP. Spektra pelepasan PL mendedahkan pelepasan biru pada 485 nm disebabkan oleh interstitial zink. Untuk semua keadaan sintesis, pelepasan PL bergantung kepada saiz zarah willemite. Penemuan dalam kajian ini memberi laluan baru untuk mengurangkan tenaga yang tinggi yang digunakan dalam sintesis nanopartikel willemite, dan tenaga jurang jalur lebar bagi bahan mungkin mempunyai aplikasi utama yang penting untuk peranti pencahayaan optoelektronik di masa depan.

ACKNOWLEDGEMENTS

All thanks and praises must be to the Almighty Allah, the most Beneficent and the most Merciful by whose power I accomplished this challenging task.

I would like to extend thanks to the following people:

First and foremost to my able supervisor Prof. Madya Dr. Khamirul Amin Matori for his tireless assistance, guidance and moral advice throughout my studies.

My sincere thanks and regards to my co-supervisors Professor Dr. Sidek Bin Hj Abd Aziz and Dr. Yazid Yaakob for their contributions in their fields of expertise.

My utmost appreciation goes to my beloved wife and our kids for their love, prayer, and understanding.

I appreciate the tremendous contributions of my brother and mentor Engr A.M Alibe.

Special appreciation goes to the Borno state governor-elect Engr Prof B.G Umara Zulum, Mni, FNSE and Distinguished Sen. Abubakar Kyari for the moral and financial support. Thank you and God bless.

I will like to acknowledge the financial support received from Petroleum Technology Development Fund (PTDF Nigeria) through the “Top-UP” scholarship number PTDF/ED/PHD/AIM/1309/17. My sincere appreciation also goes the Executive Secretary and the entire PTDF staff.

Special appreciation to National Research Institute for Chemical Technology Zaria for the study leave.

A Big thank you to Dr. Mohd Hafiz, Hhasif, Engr Bashir Inuwa, Engr Zannah, Salisu Nasir, Alhasan Y.A, Engr Abubakar S.M, Engr Mohd A.M, Dr. Dauda M.G, Ali Mohd Baba and Engr Baba Kura Zannah.

I certify that a Thesis Examination Committee has met on 18 February 2019 to conduct the final examination of Alibe Ibrahim Mustapha on his thesis entitled "Structural and Optical Properties of Willemite Nanoparticles Synthesized by Polymer Thermal Treatment Method" in accordance with the Universities and University Colleges Act 1971 and the Constitution of the Universiti Putra Malaysia [P.U.(A) 106] 15 March 1998. The Committee recommends that the student be awarded the Doctor of Philosophy.

Members of the Thesis Examination Committee were as follows:

Hishamuddin b Zainuddin, PhD

Associate Professor
Faculty of Science
Universiti Putra Malaysia
(Chairman)

Halimah bt Mohamed Kamari, PhD

Professor
Faculty of Science
Universiti Putra Malaysia
(Internal Examiner)

Zainal Abidin b Talib, PhD

Professor
Faculty of Science
Universiti Putra Malaysia
(Internal Examiner)

Lassaad El Mir, PhD

Professor
Al-Imam Mohammad Ibn Saud Islamic University
Saudi Arabia
(External Examiner)



RUSLI HAJI ABDULLAH, PhD
Professor and Deputy Dean
School of Graduate Studies
Universiti Putra Malaysia

Date: 23 April 2019

This thesis was submitted to the Senate of Universiti Putra Malaysia and has been accepted as fulfillment of the requirement for the Doctor of Philosophy. The members of the Supervisory Committee were as follows:

Khamirul Amin Matori, PhD
Associate Professor
Institute of Advanced Technology
Universiti Putra Malaysia
(Chairman)

Sidek Hj. Abd Aziz, PhD
Professor
Faculty of Science
Universiti Putra Malaysia
(Member)

Yazid Yaakob, PhD
Senior Lecturer
Faculty of Science
Universiti Putra Malaysia
(Member)

ROBIAH BINTI YUNUS, PhD
Professor and Dean
School of Graduate Studies
Universiti Putra Malaysia

Date:

Declaration by graduate student

I hereby confirm that:

- this thesis is my original work;
- quotations, illustrations and citations have been duly referenced;
- this thesis has not been submitted previously or concurrently for any other degree at any other institutions;
- intellectual property from the thesis and copyright of thesis are fully-owned by Universiti Putra Malaysia, as according to the Universiti Putra Malaysia (Research) Rules 2012;
- written permission must be obtained from supervisor and the office of Deputy Vice-Chancellor (Research and Innovation) before thesis is published (in the form of written, printed or in electronic form) including books, journals, modules, proceedings, popular writings, seminar papers, manuscripts, posters, reports, lecture notes, learning modules or any other materials as stated in the Universiti Putra Malaysia (Research) Rules 2012;
- there is no plagiarism or data falsification/fabrication in the thesis, and scholarly integrity is upheld as according to the Universiti Putra Malaysia (Graduate Studies) Rules 2003 (Revision 2012-2013) and the Universiti Putra Malaysia (Research) Rules 2012. The thesis has undergone plagiarism detection software.

Signature: 

Date: _____

Name and Matric No: Alibe Ibrahim Mustapha GS46148

Declaration by Members of Supervisory Committee

This is to confirm that:

- the research conducted and the writing of this thesis was under our supervision;
- supervision responsibilities as stated in the Universiti Putra Malaysia (Graduate Studies) Rule 2003 (Revision 2012-2013) are adhered to.

Signature: _____

Name of Chairman
of Supervisory
Committee: Associate Professor Dr. Khamirul Amin Matori

Signature: _____

Name of Member
of Supervisory
Committee: Professor Dr. Sidek Hj. Abdul Aziz

Signature: _____

Name of Member
of Supervisory
Committee: Dr. Yazid Yaakob

TABLE OF CONTENTS

	Page
ABSTRACT	i
ABSTRAK	ii
ACKNOWLEDGEMENTS	iii
APPROVAL	iv
DECLARATION	vi
LIST OF TABLES	xi
LIST OF FIGURES	xii
LIST OF ABBREVIATIONS	xix
CHAPTER	
1 INTRODUCTION	1
1.1 Research Background	1
1.2 Problem Statement	2
1.3 The significance of the study	3
1.4 Research Objective	3
1.5 Hypothesis	4
1.6 Scope of the study	4
1.7 Thesis outline	5
2 LITERATURE REVIEW	6
2.1 Nanotechnology	6
2.2 Nanomaterials and their classification	7
2.2.1 Zero-dimensional nanomaterials	8
2.2.2 One-dimensional nanomaterials	9
2.2.3 Two-dimensional nanomaterials	9
2.2.4 Three-dimensional nanomaterials	10
2.3 Techniques of nanomaterials preparation	11
2.4 Nanophosphors materials	12
2.5 Willemite Based Phosphors	13
2.5.1 Willemite Phase equilibrium	14
2.5.2 Green-emitting α -phase willemite	15
2.5.3 Yellow-emitting β -phase willemite	16
2.5.4 Red-emitting γ -phase willemite	17
2.6 Optical studies	17
2.6.1 Optical absorbance	18
2.6.2 Optical band gap	18
2.6.3 Photoluminescent	22
2.7 Applications of willemite based phosphors	23
2.8 Established synthesis methods for willemite	24
2.8.1 Conventional solid-state and sintering methods	24
2.8.2 Sol gel method	26
2.8.3 Hydrothermal Method	27

2.8.4	Super critical water method	29
2.8.5	Vapour Method	29
2.8.6	Spray pyrolysis method	31
2.8.7	Polymer thermal treatment method	32
3	MATERIALS AND METHODS	34
3.1	Introduction	34
3.1.1	Materials	34
3.1.2	Experimental Procedure	34
3.1.3	Preparation for optimum calcination temperature	34
3.1.4	Preparation for optimum calcination holding time	36
3.1.5	Preparation for optimum PVP concentration	36
3.1.6	Preparation for optimum Zn/Si concentration	36
3.2	Calcination Process	37
3.3	Characterization	37
3.3.1	Thermogravimetric analysis (TGA)	37
3.3.2	Fourier transforms infrared spectroscopy (FT–IR)	38
3.3.3	Raman spectroscopy	39
3.3.4	X–ray diffraction spectroscopy (XRD)	41
3.3.5	Field emission scanning electron microscopy (FESEM)	43
3.3.6	Energy dispersive X–ray spectroscopy (EDX)	44
3.3.7	High resolution transmission electron microscopy (HR–TEM)	45
3.3.8	Ultra violet visible spectrometer (UV–vis.)	46
3.3.9	Photoluminescence spectroscopy (PL)	47
3.4	Analysis of experimental error	48
4	RESULTS AND DISCUSSION	50
4.1	Introduction	50
4.2	Thermogravimetric analysis of PVP under different atmospheric condition	50
4.3	Effects of calcination temperature on the formation and properties of willemite nanoparticles.	54
4.3.1	XRD analysis	54
4.3.2	Functional groups and the phase composition	58
4.3.3	Raman spectroscopy analysis	61
4.3.4	Analysis of nanoparticle shape, size, and distribution	64
4.3.5	Surface morphology and elemental composition Examination	67
4.3.6	UV–vis analysis	72
4.3.7	Optical band gap analysis	73
4.3.8	Photoluminescence analysis	81
4.4	Effects of calcination holding time	82
4.4.1	XRD analysis	83
4.4.2	FT–IR Analysis	85
4.4.3	Raman spectroscopy	87
4.4.4	HR–TEM analysis.	89

4.4.5	FESEM–EDX analysis	93
4.4.6	UV–vis analysis	95
4.4.7	Optical band gap determination	96
4.4.8	Photoluminescence analysis	98
4.5	Effects of PVP concentration	99
4.5.1	Mechanism of the interaction between PVP and Precursor.	100
4.5.2	XRD analysis	101
4.5.3	FT–IR Analysis	104
4.5.4	Raman spectroscopy analysis	106
4.5.5	HR–TEM analysis	107
4.5.6	Surface morphology and elemental analysis	110
4.5.7	Optical absorbance	112
4.5.8	Optical band gap determination	113
4.5.9	Photoluminescence analysis	116
4.6	Effects of precursor concentration	118
4.6.1	XRD analysis	118
4.6.2	FTIR analysis	122
4.6.3	Raman spectroscopy analysis	125
4.6.4	HR–TEM analysis	130
4.6.5	Surface morphological analysis.	135
4.6.6	Optical absorbance properties	140
4.6.7	Optical band gap analysis	143
4.6.8	Photoluminescence analysis	147
5	CONCLUSIONS AND FUTURE WORK	151
5.1	Introduction	151
5.2	Conclusion	151
5.3	Recommendation and Future work	153
REFERENCES		154
APPENDICES		186
BIODATA OF STUDENT		196
LIST OF PUBLICATIONS		197

LIST OF TABLES

Table	Page
4.1 FT-IR absorption band and their corresponding assignments	60
4.2 Raman absorption band and their assignments	64
4.3 Comparisons of E_{opt} with different n values for willemite nanoparticles calcined at various temperatures	80
4.4 Summary of the structural and optical features of the synthesized willemite NPs calcined at 900 °C with different calcination holding time	85
4.5 Summary of the FT-IR spectra band position and their assignment	86
4.6 Comparison of the produced willemite nanoparticles obtained with other similar work	92
4.7 Variation of optical band gap energy for willemite nanoparticles calcined at 900 °C for different calcination holding time	98
4.8 Summary of the structural and optical features of the synthesized willemite NPs calcined at 900 °C with different PVP amounts	104
4.9 Summary of the impact different PVP amounts on the optical band gap of the willemite NPs synthesized at the calcination temperature of 900 °C	116
4.10 The average crystallite size (in nm) of willemite nanoparticles prepared with different ratios of Zn:Si	122
4.11 The average particles size (in nm) of willemite nanoparticles prepared with different ratios of Zn:Si	134
4.12 Summary of the impact different Zn:Si ratio on the optical band gap of the willemite nanoparticles synthesized at the calcination temperature of 900 °C	144

LIST OF FIGURES

Figure	Page
2.1 The percentage of atoms in bulk and on the surface as a function of particle size	7
2.2 SEM and TEM images of different kinds of 0D nanomaterials reported. (A) Quantum dots, (B) nanoparticles arrays, (C) core-shell nanoparticles, (D) hollow cubes, and (E) nanospheres	8
2.3 SEM micrographs of different kinds of 1D nanomaterials. (A) Nanowires, (B) nanorods, (C) nanotubes, (D) nanobelts, (E) nanoribbons, and (F) hierarchical nanostructures	9
2.4 SEM and TEM micrograph of several types of 2D nanomaterials, (A) Junctions (continuous islands), (B) branched structures, (C) nanoplates, (D) nanosheets, (E) nanowalls, and (F) nanodisk	10
2.5 Micrograph showing SEM and TEM pictures of different varieties of 3D nanomaterials, which was reported by Tiwari et al., 2012. (A) Nanoballs (dendritic structures), (B) nanocoils, (C) nanocones, (D) nanopillars, and (E) nanoflowers	11
2.6 Diagram showing two different techniques for the synthesis of nanoparticles	12
2.7 Microstructure of willemite ore	13
2.8 The ZnO–SiO ₂ –H ₂ O system. The curve between hemimorphite, and willemite is based composition of 2ZnO/SiO ₂ . The curve between pure saucnite or zincsilite and hemimorphite is based on compositions of ZnO/2SiO ₂ to 3ZnO/4SiO ₂ with excess SiO ₂	14
2.9 Equilibrium phase diagram for ZnO–SiO ₂ binary system	15
2.10 Crystalline structure of α -phase Zn ₂ SiO ₄	16
2.11 Electron transitions in a direct band gap and an indirect band gap semiconductors	21
2.12 Guest ion and their corresponding emission peaks for willemite host crystals	23
3.1 A schematic diagram for the polymer thermal treatment method	35
3.2 Schematic diagram of Interferometer	39
3.3 Schematic diagram for Raman spectroscopy	41

3.4	Schematic diagram of X-ray Diffractometer	42
3.5	Schematic diagrams for the principle of UV-vis spectroscopy	46
3.6	Schematic diagrams for the principle of Photoluminescence spectroscopy adapted from	48
4.1	TG-DTG curves for the decomposition of PVP at a heating rate of 10 °C/min under nitrogen atmosphere	51
4.2	TG-DTG curves for the decomposition of PVP at a heating rate of 10 °C/min under oxygen atmosphere	52
4.3	TG-DTG curves for the decomposition of PVP at a heating rate of 10 °C/min under air atmosphere	53
4.4	TG-DTG curves for the decomposition of PVP at a heating rate of 10 °C/min without passing any gas	54
4.5	X-ray diffraction of the uncalcined sample at room temperature.	56
4.6	XRD patterns of willemite nanoparticles at different calcination temperatures between the range 500–1000 °C	57
4.7	FT-IR spectrum of the sample before the calcination process.	59
4.8	FT-IR spectra of willemite nanoparticles calcined: (a) 500 °C, (b) 600 °C, (c) 700 °C, (d) 800 °C, (e) 900°C and (f) 1000 °C in the range of 200–4000 cm ⁻¹	60
4.9	Raman spectrum of the sample before the calcination process.	62
4.10	Raman spectra of willemite nanoparticles calcined at different temperatures: (a) 500, (b) 600, (c) 700, (d) 800, (e) 900 and (f) 1000 °C in the range of 200–4000 cm ⁻¹	63
4.11	TEM analysis of willemite nanoparticles calcined at different temperatures: (a) 500, (b) 600, (c) 700, (d) 800, (e) 900, and (f) 1000 °C	65
4.12	Nanoparticles size distribution of willemite calcined at different temperatures: (a) 500 °C, (b) 600 °C, (c) 700 °C, (d) 800 °C, (e) 900 °C, and (f) 1000 °C	66
4.13	FESEM micrographs of the samples calcined at different temperatures	68
4.14	EDX spectrums of sample calcined at 500 °C	69
4.15	EDX spectrums of sample calcined at 600 °C	69

4.16	EDX spectrums of sample calcined at 700 °C	70
4.17	EDX spectrums of sample calcined at 800 °C	70
4.18	EDX spectrums of sample calcined at 900 °C	71
4.19	EDX spectrums of sample calcined at 1000 °C	71
4.20	UV-vis absorption spectra of the willemite nanoparticles calcined at various temperatures	72
4.21	Plot of extinction coefficient versus photon energy (hv) for willemite nanoparticles calcined at 500 °C	74
4.22	Plot of extinction coefficient versus photon energy (hv) for willemite nanoparticles calcined at 600 °C	74
4.23	Plot of extinction coefficient versus photon energy (hv) for willemite nanoparticles calcined at 700 °C	75
4.24	Plot of extinction coefficient versus photon energy (hv) for willemite nanoparticles calcined at 800 °C	75
4.25	Plot of extinction coefficient versus photon energy (hv) for willemite nanoparticles calcined at 900 °C	76
4.26	Plot of extinction coefficient versus photon energy (hv) for willemite nanoparticles calcined at 1000 °C	76
4.27	Plot of $(\alpha h\nu)^{1/n}$ as a function of photon energy (hv) for willemite nanoparticles calcined at 500 °C	77
4.28	Plot of $(\alpha h\nu)^{1/n}$ as a function of photon energy (hv) for willemite nanoparticles calcined at 600 °C	77
4.29	Plot of $(\alpha h\nu)^{1/n}$ as a function of photon energy (hv) for willemite nanoparticles calcined at 700 °C	78
4.3	Plot of $(\alpha h\nu)^{1/n}$ as a function of photon energy (hv) for willemite nanoparticles calcined at 800 °C	78
4.31	Plot of $(\alpha h\nu)^{1/n}$ as a function of photon energy (hv) for willemite nanoparticles calcined at 900 °C	79
4.32	Plot of $(\alpha h\nu)^{1/n}$ as a function of photon energy (hv) for willemite nanoparticles calcined at 1000 °C	79
4.33	PL spectra of Willemite nanoparticles under the excitation wavelength of 350 nm calcined at (a) 500 °C, (b) 600 °C, (c) 700 °C, (d) 800 °C, (e) 900 °C and (f) 1000 °C	82

4.34	X-ray diffraction of (a) uncalcined sample and willemite nanoparticles calcined at 900 °C over a range of calcination holding time of (b) 1 h, (c) 2 h, (d) 3 h and (e) 4 h	84
4.35	XRD reference patterns of willemite nanoparticles synthesized at the optimum synthesis condition of 900 °C/3 h (Masjedi–Arani, and Salavati–Niasari, 2016)	84
4.36	FT–IR spectra of (a) uncalcined sample and willemite nanoparticles calcined at 900 °C over a range of calcination holding times of (b) 1 h, (c) 2 h, (d) 3 h and (e) 4 h	86
4.37	Raman spectra of (a) uncalcined sample and willemite NPs calcined at 900 °C over a range of calcination holding time of (b) 1 h, (c) 2 h, (d) 3 h and (e) 4 h	88
4.38	HR–TEM micrographs and the corresponding lattice measurement for willemite nanoparticles produced at 900 °C produced at various calcination holding time: (a, a') 1 h, (b, b') 2 h , (c, c') 3 h, and (d, d') 4 h	90
4.39	Particle size distribution of willemite nanoparticles calcined at 900 °C for several holding time (a) 1 h, (b) 2 h, (c) 3 h and (d) 4 h.	91
4.40	FESEM showing Micrograph for willemite nanoparticles produced at 900 °C with different calcination holding time: (a) 1 h, (b) 2 h, and (c) 3 h and (d) 4 h	94
4.41	EDX spectrum of willemite nanoparticles calcined at 900 °C with different calcination holding time: (a) 1 h, (b) 2 h, (c) 3 h and (d) 4 h	94
4.42	Optical absorbance spectra of the willemite nanoparticles produced at 900 °C with different calcination holding time: (a) 1 h, (b) 2 h, (c) 3 h and (d) 4 h	95
4.43	(a) The experimental optical band gap using extinction coefficient and (b) Optical band gap from Mott and Davis Model for $n = 1/2$ transition	97
4.44	PL spectra of willemite nanoparticles calcined at 900 °C at different calcination holding times: (a) 1 h, (b) 2 h, (c) 3 h, (d) 4 h	99
4.45	A proposed mechanism of interaction for metal ions and PVP in the of formation willemite nanoparticles	100
4.46	XRD patterns of willemite nanoparticles obtained following calcination involving a range of PVP concentration. (a) 0 g (b) PVP 30 °C (c) 2 g, (d) 3 g (e) 4 g, (f) 5 g	102

4.47	XRD reference patterns of: (a) willemite nanoparticles produced at 900 °C: (a) 0 g in the absence of PVP, (b) 4 g PVP concentration	103
4.48	FT-IR spectra of willemite NPs over a range of PVP amounts: (a) Different amounts of PVP at 30 °C, (b) 2 g, (c) 3 g, (d) 4 g, (e) 5 g	105
4.49	Raman spectra of willemite nanoparticles calcined at 900 °C over a range of PVP amounts (a) 2 g, (b) 3 g, (c) 4 g, (d) 5 g	106
4.50	TEM images of willemite nanoparticles and the corresponding lattice measurement and SAED at PVP different concentration of (a-c) 0 g, (d-f) 2 g, (g-i) 3 g, and (j-l) 4 g, (m-o) 5 g	108
4.51	Particle size distribution of willemite nanoparticles calcined at 800 °C at PVP different concentration: (a) 2 g, (b) 3 g, (c) 4 g and (d) 5 g	109
4.52	FESEM images of willemite nanoparticles following calcination at 900 °C over PVP different concentration of (a) 0 g, (c) 2 g, (c) 3 g, and (c) 4 g, (d) 5 g	111
4.53	EDX spectrum of willemite nanoparticles calcined 900 °C, over a range PVP concentration of (a) 2 g, (b) 3 g, (c) 4 g, and (d) 5 g	112
4.54	The Optical absorbance spectra of the willemite nanoparticles over a range of PVP amounts: (a) 2 g, (b) 3 g, (c) 4 g, and (d) 5 g	113
4.55	Plot of extinction coefficient versus photon energy ($h\nu$) for willemite nanoparticle calcined at 900 °C for various PVP amounts	114
4.56	Plot of $(\alpha h\nu)^{1/2}$ as a function of photon energy ($h\nu$) for willemite nanoparticles calcined at 900 °C for various PVP amounts	115
4.57	PVP Compositional dependence of experimental optical band gap and optical band gap from Mott and Davis Model for $n = 1/2$ transition	115
4.58	PL spectra of the willemite nanoparticles under 350 nm excitation wavelength for various PVP amounts (a) 2 g, (b) 3 g, (c) 4 g, (d) 5 g	117
4.59	XRD pattern of Zn:Si ratio for 1:1 calcined between 700 to 1000 °C	120
4.60	XRD pattern of Zn:Si ratio for 1.5:1 calcined between 700 to 1000 °C	120
4.61	XRD pattern of Zn:Si ratio for 2:1 calcined between 700 to 1000 °C	121
4.62	XRD pattern of Zn:Si ratio for 3:1 calcined between 700 to 1000 °C	121
4.63	FTIR pattern of Zn:Si ratio of 1:1, calcined between 700 to 1000 °C	123
4.64	FTIR pattern of Zn:Si ratio of 1.5:1, calcined between 700 to 1000 °C	123

4.65	FTIR pattern of Zn:Si ratio of 2:1, calcined between 700 to 1000 °C	124
4.66	FTIR pattern of Zn:Si ratio of 3:1, calcined between 700 to 1000 °C	124
4.67	Raman spectra for sample with Zn:Si ratio of 1:1 calcined between 700–1000 °C	126
4.68	Raman spectra for sample with Zn:Si ratio of 1.5:1 calcined between 700–1000 °C	127
4.69	Raman spectra for sample with Zn:Si ratio of 2:1 calcined between 700–1000 °C	128
4.70	Raman spectra for sample with Zn:Si ratio of 3:1 calcined between 700–1000 °C	129
4.71	HR–TEM micrographs of willemite nanoparticles with Zn:Si ratio of 1:1, calcined at: (a) 800 °C, (b) 900 °C, (c) 1000 °C	131
4.72	HR–TEM micrographs of willemite nanoparticles with Zn:Si ratio of 1.5:1, calcined at: (a) 800 °C, (b) 900 °C, (c) 1000 °C	132
4.73	HR–TEM micrographs of willemite nanoparticles with Zn:Si ratio of 2:1, calcined at: (a) 800 °C, (b) 900 °C, (c) 1000 °C	133
4.74	HR–TEM micrographs of willemite nanoparticles with Zn:Si ratio of 3:1, calcined at: (a) 800 °C, (b) 900 °C, (c) 1000 °C	134
4.75	FESEM micrographs of willemite nanoparticles with Zn:Si ratio of 1:1, calcined at: (a) 800 °C, (b) 900 °C, (c) 1000 °C	136
4.76	FESEM micrographs of willemite nanoparticles with Zn:Si ratio of 1.5:1, calcined at: (a) 800 °C, (b) 900 °C, (c) 1000 °C	137
4.77	FESEM micrographs of willemite nanoparticles with Zn:Si ratio of 2:1, calcined at: (a) 800 °C, (b) 900 °C, (c) 1000 °C	138
4.78	FESEM micrographs of willemite nanoparticles with Zn:Si ratio of 3:1, calcined at: (a) 800 °C, (b) 900 °C, (c) 1000 °C	139
4.79	The Optical absorbance spectra of the willemite nanoparticles with Zn:Si ratio of 1:1, calcined between 800–1000 °C	141
4.80	The Optical absorbance spectra of the willemite nanoparticles with Zn:Si ratio of 1.5:1, calcined between 800–1000 °C	141
4.81	The Optical absorbance spectra of the willemite nanoparticles with Zn:Si ratio of 2:1, calcined between 800–1000 °C	142

4.82	The Optical absorbance spectra of the willemite nanoparticles with Zn:Si ratio of 3:1, calcined between 800–1000 °C	142
4.83	Plot of extinction coefficient versus photon energy ($h\nu$) for willemite nanoparticle calcined at 900 °C for various Zn:Si ratio; (a) 1:1, (b) 1.5:1, (c) 2:1, and (d) 3:1	144
4.84	Plot of $(\alpha h\nu)^{1/n}$ as a function of photon energy ($h\nu$) for willemite nanoparticles with Zn:Si ratio 1:1 calcined at 900 °C	145
4.85	Plot of $(\alpha h\nu)^{1/n}$ as a function of photon energy ($h\nu$) for willemite nanoparticles with Zn:Si ratio 1.5:1 calcined at 900 °C	145
4.86	Plot of $(\alpha h\nu)^{1/n}$ as a function of photon energy ($h\nu$) for willemite nanoparticles with Zn:Si ratio 2:1 calcined at 900 °C	146
4.87	Plot of $(\alpha h\nu)^{1/n}$ as a function of photon energy ($h\nu$) for willemite nanoparticles with Zn:Si ratio 3:1 calcined at 900 °C	146
4.88	PL spectra of the willemite nanoparticles under 350 nm excitation wavelength for Zn:Si ratio 1:1	148
4.89	PL spectra of the willemite nanoparticles under 350 nm excitation wavelength for Zn:Si ratio 1.5:1	149
4.90	PL spectra of the willemite nanoparticles under 350 nm excitation wavelength for Zn:Si ratio 2:1	149
4.91	PL spectra of the willemite nanoparticles under 350 nm excitation wavelength for Zn:Si ratio 3:1	150

LIST OF ABBREVIATIONS

CB	Conduction band
DCCAs	Drying control chemical additives
D.I	Deionized
E_{opt}	Optical band gap
FESEM	Field Electron Scanning Microscopy
FT-IR	Fourier Transforms Infrared Spectroscopy
HCl	Hydrochloric acid
HR-TEM	High Resolution transmission electron microscopy
JCPDS	Joint Committee on Powder Diffraction Standards
KM	Kubelka-Munk
NPs	Nanoparticles
PL	Photoluminescent
PBNM	Phosphors based nanomaterials
PEG	Polyethylene glycol
PVA	Polyvinyl pyrrolidone alcohol
PVP	Poly(vinyl pyrrolidone),
SLS	Soda lime silica
TGA	Thermogravimetric analysis
VB	Valence band
UV	Ultraviolet
UV-vis	Ultraviolet-visible spectroscopy
XRD	X-ray diffraction

CHAPTER 1

INTRODUCTION

1.1 Research Background

Phosphors based nanomaterials (PBNM) have demonstrated a substantial interest from scientist and researchers in several fields across the globe, due to their attractive physical and chemical properties (Horikoshi and Serpone, 2013). Nanomaterials such as the PBNM offers exceptional properties like quantum confinement effects couple with an increased surface area to volume ratio (Chander, 2005). These properties uniquely differentiate them from those in their bulk amount (Wu et al., 2002).

PBNM are studied broadly for numerous interdisciplinary applications (Alivisatos, 1996; Klimov et al., 2000; Chandan et al., 2018; Garakyanaghi and Castellano, 2018). Conceivably, the most interesting characteristic of these materials, from both an academic research point of view and at an industrial standpoint, is their unique size-dependent electronic nature, the ability to create structure and devices with tailor-made electronic characteristics by modifying the size of one of the constituent materials (Norris and Bawendi, 1996; Chen et al., 2017). Most often, the properties of PBNM are treated with other materials of interest in a system or device; for instance, functionalization of PBNM with biomolecules for medical imaging (Kairdolf et al., 2017; McHugh et al., 2018); creating nanostructured electronic arrays by linking several PBNM with short-chain molecules (Talapin et al., 2009; Gupta et al., 2018); producing fine nanoparticles for optoelectronic displays and sensors devices (Coe-Sullivan, 2009; Chen et al., 2018); or synthesizing PBNM systems with other semiconducting material to form cheaper next-generation photovoltaic devices (Selopal et al., 2016; Zhao et al., 2016). In each of the applications above, PBNM are exploited for their size-dependent electronic structure. Zinc silicate or willemite, for instance, is considered to be one of the earlier identified as the naturally occurring PBNM for phosphors applications. Inorganic material especially in nano-form like the willemite nanoparticles are considered to be a good host for phosphor ions because of their chemical and physical properties and have attracted attraction researcher's interest (Takesue et al., 2009).

Willemite is associated with the wide band gap oxide based materials (Omri et al., 2013; El Mir and Omri, 2014; Bharti et al., 2018; Omri et al., 2017). Willemite exists as naturally occurring minerals combined with the little number of zinc ores exhibiting a phenacite structure in which Zn–O tetrahedral shares corners with Si–O tetrahedral thus making hollow tubes appearing parallel to the plane [0001] (Klaska et al., 1978, Chang et al., 1999). This structure is a rigid lattice which enables the atoms to conquer the whole position and composed of the tetrahedral structure.

Having possessing this structure, willemite offers distinguished chemical and physical characteristics (Takesue et al., 2009). In light of this, willemite become one of the famous green phosphor material in optical and lighting devices and laser crystals applications (Veremeichik et al., 2003; Wan et al., 2005; Yu and Wang, 2009; Zaid et al., 2016; Vitkin et al., 2017; El Mir and Omri, 2018; Onufrieva et al., 2018). Willemite additional potentials applications include but not limited to, their usage as an adsorbents (Wang et al., 2012; Dai et al., 2017), optoelectronics application (Zaid et al., 2016; Effendy et al., 2017), and photonic devices (Romanov et al., 2000; Tarafder et al., 2016).

Furthermore, willemite is fame for its suitability serving as good host material used for several guest ions of rare-earth and transitional metal to attain higher effectiveness in displaying wider range of multi-colours for luminescence application (Omri et al., 2013; El Mir and Omri, 2014; Al-Nidawi et al., 2017; Effendy et al., 2017; Zaid et al., 2016; Omar et al., 2017; Omar et al., 2016; Rasdi et al., 2017;). For instance, the luminescence characteristics of rare earth ions (RE^{3+}) like the long emission lifetime, sharper luminescence array and the characteristic spectral behavior as they are filled by 4f shells and shielded by the outer $5s^2$ and $5p^6$ orbitals are some of the motivating drivers for their choice in nowadays optoelectronic application. For this reason, willemite doped with RE^{3+} is creating major attention for its luminescence efficiency and colour purity for lighting devices (Omar et al., 2017). Furthermore, Takesue et al. (2009) reported the optical performance of willemite doped manganese ($\text{Zn}_2\text{SiO}_4:\text{Mn}^{2+}$) phosphors where the $3d^5$ electron transition in Mn^{2+} ions is characterized as activating centre in the Zn_2SiO_4 structure. The strong green emission obtained under Ultraviolet light is directly due to the excitation from the lowest state ${}^4\text{T}_1(\text{G})$ to ${}^6\text{A}_1(\text{S})$ of the ground state (Lukić et al 2008; Uegaio et al., 2012; Park et al., 2015).

1.2 Problem Statement

The earth is globally faced with tough environmental dreadful degradations and energy resources because of continues usage of conventional fossil fuels which lead to the greenhouse effects. The great challenges of the 21st century are undoubtedly the need to create a system that reduces high energy consumption and carbon gas emission to the environment. Manufacturing industries including phosphor industry have been criticized for higher energy consumption and greenhouse gases emission, attributed to the high temperature of production (Zhang and Cheng, 2009; Canadell and Raupach, 2008). In recent years, willemite based phosphors are fascinating a remarkable attention in optical, and lighting devices (Omar et al., 2017; Rasdi et al., 2017; Mbule et al., 2017; Dang et al., 2018; Nakamura et al., 2018; Omri et al., 2018; Wei et al., 2018; Zaitseva et al., 2018). Willemite nanoparticles have previously been produced using several synthesis techniques such as the conventional sol-gel and solid state techniques. Other established methods include combustion method, a mechanical method, hydrothermal method, spray pyrolysis method wet-chemical method, and microwave method. However, most of these methods have some setback that is limiting their choices, such as high production

temperature involved, complexity in procedures, the lengthier period for the reaction to take part, poisonous substances and a harmful effluent that are possibly detrimental to the environments. In light of the reason above, this study is focused on developing new environmental friendly synthesis technique, yet simple and low cost effective for producing willemite nanoparticles. Polymer thermal treatment method offers a remedy and to curb the drawback of the previous methods of synthesis. The study investigates the effects of the synthesis conditions on the formation and properties of these willemite nanoparticles by polymer thermal treatment method and followed by the characterization of their properties. The findings in this study are anticipated to find a potential application as phosphor material for optoelectronic devices.

1.3 The significance of the study

In recent times, willemite nanomaterials open greater prospects for creating new materials and fascinating an essential interest in phosphors and optoelectronic. A higher attention of research have been pointed on the production of willemite nanoparticles to achieve useful luminescent materials for oscilloscopes, multi-color light emitting diode and several displays panels and lighting devices (Takesue et al., 2009; Ding et al., 2015)

Willemite has been considered suitable phosphor host matrix for several guest ions such as rare earth and transitional metal as dopant ions for effective optical performance (Azman et al., 2018; Omri et al., 2018). The structure in willemite is such that the entire atoms occupying the overall position and made up of the tetrahedral structure where zinc and silicon are placed in three different fourfold crystallographic sites. Thus, such rigid lattice provides the chances to attain improved optical properties (Takesue et al., 2009; Tarafder et al., 2014).

To the best of the author's knowledge, there are not yet available literature reports on the production of willemite based phosphor using a polymer thermal treatment technique. Thus, this work presents an optimized production of willemite nanoparticles by controlling parameters like calcination temperature and holding times, precursor and PVP concentration. Consequently, the enhanced structural and optical properties of the materials may be possible as a candidate for optoelectronics devices applications.

1.4 Research Objective

This study aims to fabricate and optimize willemite nanoparticles by polymer thermal treatment method. This project employs the design of appropriate metallic precursor and polymer compositions, development of the calcination process, a series of fundamental studies on the willemite crystallization and formation process.

This study was conducted based on the following objectives:

- 1) To determine the effects of calcination temperature on the formation, structural and optical properties of the willemite nanoparticles
- 2) To examine the effects of the calcination holding time on the formation, structural and optical properties of the willemite nanoparticles.
- 3) To study the influence of PVP concentrations on the formation, structural and optical properties of the willemite nanoparticles.
- 4) To investigate the impact of precursors concentrations on the formation, structural and optical properties of the willemite nanoparticles.

1.5 Hypothesis

Polymer thermal treatment method will reduce the problems involves in high calcination temperature and the use of lethal chemical reagent and large agglomeration in the production of willemite nanoparticles. The purity of the willemite nanoparticles produced depends on the interaction between the metallic ions and a capping agent (PVP) that undergo to the calcination process which causes the nucleation and growth of the nanoparticles. In this technique, the role of PVP is to stabilize the metallic ions, so that the agglomeration of the nanoparticles could be diminished. Higher concentration of the PVP leads to more capping ability, and produced smaller nanoparticles. Consequently, the optical properties of the willemite nanoparticles produced such as the wide band gap energy may have possible applications for future semiconductor lighting devices.

1.6 Scope of the study

This work is limited to the stated aim and objective which is the production of willemite nanoparticles by polymer thermal treatment method only. In the present study, willemite nanoparticles were synthesized by the polymer thermal treatment method considering several synthesis parameters such as calcination temperature and holding times, the concentration of the metal precursor and the polymer effects. Apart from that, the influence of these parameters on the microstructural, morphological and optical characteristics of the willemite nanoparticles was as well lengthily studied and discussed. The investigation of other properties like dielectric, photocatalytic, and magnetic properties of willemite nanoparticles did not fall within the scope of the study.

To realize the stated objective, the following are considered as the scopes of the study:

- 1) A series of metallic precursor of zinc acetate dihydrate and silicon tetraacetate ($\text{Zn}(\text{CH}_3\text{COO})_2 \cdot 2\text{H}_2\text{O}$ and $\text{Si}(\text{OCOCH}_3)_4$) with several concentration based on the stoichiometric molar ratio of Zn:Si, 1:1, 1.5:1, 2:1 and 3:1 has been used to prepare willemite nanoparticles, while keeping the PVP concentration constant.
- 2) Several PVP concentrations between 0–5 g in 100 ml of deionized water were used to obtain the optimum polymer concentration in the synthesis of the material.
- 3) The thermal decomposition and degradation properties of metallic precursor embedded in PVP before the calcination process has been measured using thermogravimetric analysis and differential thermal analysis (TGA–DTA) spectroscopy.
- 4) The structural and crystallinity of willemite based phosphor has been analyzed using XRD, HR–TEM, FESEM, Raman, and FT–IR spectroscopy.
- 5) The optical properties of willemite based phosphor have been analyzed using UV–Vis and PL spectroscopy.

1.7 Thesis outline

Synthesis and characterization of willemite nanoparticles by polymer thermal treatment method are the central focus and features of assessment in this study. Chapter 1 of this thesis consists of a brief background on phosphors based nanomaterials and willemite based phosphors. Other features in Chapter 1 includes the problem statement, the significance of the study, the research objectives, scope of the study and the thesis outline. The review of the previous literature reported on the production of willemite based phosphors, metal oxide nanoparticles by other researchers are covered in Chapter 2. The materials and tools used in the experiment, in addition to the detailed description of the procedure for the production of willemite based phosphor are discussed in Chapter 3. The results discussion on the effect of metallic precursor and PVP concentration, the progression of calcination temperatures and various proportion cerium doping amount on the structural and optical properties of the willemite based phosphor are studied in Chapter 4. The research conclusion and recommendations for possible future works are stated in Chapter 5. The last part of the thesis contains a list of references, publications, and conferences attended by the author.

REFERENCES

- Alagarasi, A. (2011). Introduction to nanomaterials. *National Center for Environmental Research (NCCR) internal bulletin*. Chennai, India.
- Al-Ani, S. K. J., Hogarth, C. A., and El-Malawany, R. A. (1985). A study of optical absorption in tellurite and tungsten–tellurite glasses. *Journal of Materials Science*, 20(2), 661–667.
- Al-Hada, N. M., Saion, E. B., Shaari, A. H., Kamarudin, M. A., Flaifel, M. H., Ahmad, S. H., and Gene, S. A. (2014). A facile thermal–treatment route to synthesize ZnO nanosheets and effect of calcination temperature. *PloS One*, 9(8), e103134.
- Al-Hada, N. M., Saion, E., Talib, Z. A., and Shaari, A. H. (2016). The impact of polyvinylpyrrolidone on properties of cadmium oxide semiconductor nanoparticles manufactured by heat treatment technique. *Polymers*, 8(4), 113.
- Ali, A. M., Ismail, A. A., Najmy, R., and Al-Hajry, A. (2014). Preparation and characterization of ZnO–SiO₂ thin films as highly efficient photocatalyst. *Journal of Photochemistry and Photobiology A: Chemistry*, 275, 37–46.
- Ali, E. A. G. E., Matori, K. A., Saion, E., Ab Aziz, S. H., Zaid, M. H. M., and Alibe, I. M. (2018). Effect of sintering temperatures on structural and optical properties of ZnO–Zn₂SiO₄ composite prepared by using amorphous SiO₂ nanoparticles. *Journal of the Australian Ceramic Society*, 54(2), 1–8.
- Alivisatos, A. P. (1996). Semiconductor clusters, nanocrystals, and quantum dots. *Science*, 271(5251), 933–937.
- Al-Nidawi, A. J. A., Matori, K. A., Zakaria, A., and Zaid, M. H. M. (2017). Effect of MnO₂ doped on physical, structure and optical properties of zinc silicate glasses from waste rice husk ash. *Results in Physics*, 7, 955–961.
- Amekura, H., Kono, K., Kishimoto, N., and Buchal, C. (2006). Formation of zinc–oxide nanoparticles in SiO₂ by ion implantation combined with thermal oxidation. *Nuclear Instruments and Methods in Physics Research Section B: Beam Interactions with Materials and Atoms*, 242(1), 96–99.
- An, J. S., Noh, J. H., Cho, I. S., Roh, H. S., Kim, J. Y., Han, H. S., and Hong, K. S. (2010). Tailoring the morphology and structure of nanosized Zn₂SiO₄:Mn²⁺ phosphors using the hydrothermal method and their luminescence properties. *The Journal of Physical Chemistry C*, 114(23), 10330–10335.
- Azman, A. Z. K., Matori, K. A., Ab Aziz, S. H., Zaid, M. H. M., Wahab, S. A. A., and Khadir, R. E. M. (2018). Comprehensive study on structural and optical properties of Tm₂O₃ doped zinc silicate based glass–ceramics. *Journal of Materials Science: Materials in Electronics*, 29(23), 19861–19866.

- Babu, B. C., and Buddhudu, S. (2014). Analysis of structural and electrical properties of Ni^{2+} : Zn_2SiO_4 ceramic powders by sol–gel method. *Journal of Sol–Gel Science and Technology*, 70(3), 405–415.
- Babu, B. C., Kumar, K. N., Rudramadevi, B. H., and Buddhudu, S. (2014). Synthesis, Structural and Dielectric Properties of Co^{2+} , Ni^{2+} and Cu^{2+} : Zn_2SiO_4 Nanoceramics by a Sol–gel Method. *Ferroelectrics Letters Section*, 41(1–3), 28–43.
- Babu, B. C., Rao, B. V., Ravi, M., and Babu, S. (2017). Structural, microstructural, optical, and dielectric properties of Mn^{2+} :Willemite Zn_2SiO_4 nanocomposites obtained by a sol–gel method. *Journal of Molecular Structure*, 1127, 6–14.
- Babu, B. C., Vandana, C. S., Guravamma, J., Rudramadevi, B. H., and Buddhudu, S. (2015). Photoluminescence analysis of Ce^{3+} : Zn_2SiO_4 and Li^{+} Ce^{3+} : Zn_2SiO_4 : phosphors by a sol–gel method. In *AIP Conference Proceedings* 1665(1), 140060.
- Babu, B. C., Wang, G.G., Yan, B., Yang, Q., and Baker, A. P. (2018). Effects of Cr^{3+} addition on the structure and optical properties of α - Zn_2SiO_4 synthesized by sol–gel method. *Ceramics International*, 44(1), 938–946.
- Babu, K. S., Reddy, A. R., and Reddy, K. V. (2014). Controlling the size and optical properties of ZnO nanoparticles by capping with SiO_2 . *Materials Research Bulletin*, 49, 537–543.
- Babu, K. S., Reddy, A. R., Reddy, K. V., and Mallika, A. N. (2014). High thermal annealing effect on structural and optical properties of ZnO – SiO_2 nanocomposite. *Materials Science in Semiconductor Processing*, 27, 643–648.
- Babu, K. S., Reddy, A. R., Sujatha, C. H., and Reddy, K. V. (2013). Effects of precursor, temperature, surface area and excitation wavelength on photoluminescence of ZnO /mesoporous silica nanocomposite. *Ceramics International*, 39(3), 3055–3064.
- Baqer, A. A., Matori, K. A., Al–Hada, N. M., Kamari, H. M., Shaari, A. H., Saion, E., and Chyi, J. L. Y. (2018). Copper oxide nanoparticles synthesized by a heat treatment approach with structural, morphological and optical characteristics. *Journal of Materials Science: Materials in Electronics*, 29(2), 1025–1033.
- Baqer, A. A., Matori, K. A., Al–Hada, N. M., Shaari, A. H., Saion, E., and Chyi, J. L. Y. (2017). Effect of polyvinylpyrrolidone on cerium oxide nanoparticle characteristics prepared by a facile heat treatment technique. *Results in Physics*, 7, 611–619.
- Basavaraj, R. B., Nagabhushana, H., Prasad, B. D., Sharma, S. C., Prashantha, S. C., and Nagabhushana, B. M. (2015). A single host white light emitting

- $\text{Zn}_2\text{SiO}_4:\text{Re}^{3+}$ (Eu, Dy, Sm) phosphor for LED applications. *Optik–International Journal for Light and Electron Optics*, 126(19), 1745–1756.
- Bell, D. C., and Garratt-Reed, A. J. (2003). *Energy dispersive X-ray analysis in the electron microscope*. Garland Science, London, United Kingdom.
- Bell, J. E., and Hall, C. (2018). UV and visible absorbance spectroscopy. In *Spectroscopy in biochemistry* (pp.3–62). CRC Press, New York, USA.
- Betti, N. A. (2016). Thermogravimetric analysis on PVA/PVP blend under air atmosphere. *Engineering and Technology Journal*, 34(13), 2433–2442.
- Bharti, D. K., Gupta, M. K., and Srivastava, A. K. (2018). Giant dielectric constant and band gap reduction in hydrothermal grown highly crystalline zinc silicate nanorods. *Materials Letters*, 232, 66–69.
- Bhatkar, V. B., Omanwar, S. K., and Moharil, S. V. (2007). Combustion synthesis of silicate phosphors. *Optical Materials*, 29(8), 1066–1070.
- Bianco, G., Soldi, M. S., Pinheiro, E. A., Pires, A. T. N., Gehlen, M. H., and Soldi, V. (2003). Thermal stability of poly (N-vinyl-2-pyrrolidone-co-methacrylic acid) copolymers in inert atmosphere. *Polymer Degradation and Stability*, 80(3), 567–574.
- Bigham, A., Foroughi, F., Motamedi, M., and Rafienia, M. (2018). Multifunctional nanoporous magnetic zinc silicate– ZnFe_2O_4 core–shell composite for bone tissue engineering applications. *Ceramics International*, 44(10), 11798–11806.
- Billstrand, B., Bian, K., Karler, C., and Fan, H. (2018). Functionalized Block-Copolymer Templates for Synthesis and Shape Control of Quantum Dots. *MRS Advances*, 3(41), 1–5.
- Biswas, A., Wang, T., and Biris, A. S. (2010). Single metal nanoparticle spectroscopy: optical characterization of individual nanosystems for biomedical applications. *Nanoscale*, 2(9), 1560–1572.
- Boni, M., and Large, D. (2003). Nonsulfide zinc mineralization in Europe: An overview. *Economic Geology*, 98(4), 715–729.
- Bouvy, C., Marine, W., and Su, B.L. (2007). ZnO /mesoporous silica nanocomposites prepared by the reverse micelle and the colloidal methods: Photoluminescent properties and quantum size effect. *Chemical Physics Letters*, 438(1–3), 67–71.
- Braslavsky, S. E. (2007). Glossary of terms used in photochemistry, (IUPAC Recommendations 2006). *Pure and Applied Chemistry*, 79(3), 293–465.

- Broberg, D., Medasani, B., Zimmermann, N. E., Yu, G., Canning, A., Haranczyk, M., and Hautier, G. (2018). PyCDT: A Python toolkit for modeling point defects in semiconductors and insulators. *Computer Physics Communications*, 226, 165–179.
- Brown, F. C., Bi, Y., Chopra, S., Hristovski, K. D., Westerhoff, P., and Theis, T. L. (2018). End-of-Life Heavy Metal Releases from Photovoltaic Panels and Quantum Dot Films: Hazardous Waste Concerns or Not? *ACS Sustainable Chemistry and Engineering*, 6(7), 9369–9374
- Brown, J. S. (1936). Supergene sphalerite, galena, and willemite at Balmat, New York. *Economic Geology*, 31(4), 331–354.
- Brugger, J., McPhail, D. C., Wallace, M., and Waters, J. (2003). Formation of willemite in hydrothermal environments. *Economic Geology*, 98(4), 819–835.
- Brus, L. E. (1984). Electron-electron and electron-hole interactions in small semiconductor crystallites: The size dependence of the lowest excited electronic state. *The Journal of Chemical Physics*, 80(9), 4403–4409.
- Bunting, E. N. (1930). Phase Equilibria in the System Cr₂O₃–SiO₂. *Bur. Standards J. Research*, 5(2), 325–27.
- Bunting, Elmer Newman. (1930). Phase Equilibria in the System SiO₂–ZnO₁. *Journal of the American Ceramic Society*, 13(1), 5–10.
- Burova, L. I., Petukhov, D. I., Eliseev, A. A., Lukashin, A. V., and Tretyakov, Y. D. (2006). Preparation and properties of ZnO nanoparticles in the mesoporous silica matrix. *Superlattices and Microstructures*, 39(1–4), 257–266.
- Cahn, R. W., and Lifshitz, E. M. (2016). *Concise encyclopedia of materials characterization*, Pergamon Press Ltd, New York, USA.
- Canadell, J. G., and Raupach, M. R. (2008). Managing forests for climate change mitigation. *Science*, 320(5882), 1456–1457.
- Chamberlin, R. R., and Skarman, J. S. (1966). Chemical spray deposition process for inorganic films. *Journal of the Electrochemical Society*, 113(1), 86–89.
- Chandan, H. R., Schiffman, J. D., and Balakrishna, R. G. (2018). Quantum dots as fluorescent probes: Synthesis, surface chemistry, energy transfer mechanisms, and applications. *Sensors and Actuators B*, 258, 1191–1214.
- Chander, H. (2005). Development of nanophosphors—A review. *Materials Science and Engineering: R: Reports*, 49(5), 113–155.
- Chander, H. (2006). A review on synthesis of nanophosphors—Future luminescent materials. In *Proceedings of ASID*, 8–12.

- Chandrappa, G. T., Ghosh, S., and Patil, K. C. (1999). Synthesis and Properties of Willemite, Zn_2SiO_4 , and $M^{2+}:Zn_2SiO_4$ ($M=Co$ and Ni). *Journal of Materials Synthesis and Processing*, 7(5), 273–279.
- Chang, H. J., Park, H. D., Sohn, K. S., and Lee, J. D. (1999). Electronic structure of Zn_2SiO_4 and $Zn_2SiO_4:Mn$. *Journal of the Korean Physical Society*, 34(6), 545–548.
- Chaware, V., Deshmukh, R., Sarode, C., Gokhale, S., and Phatak, G. (2015). Low-temperature sintering and microwave dielectric properties of Zn_2SiO_4 ceramic added with crystalline zinc borate. *Journal of Electronic Materials*, 44(7), 2312–2320.
- Chen, B., Pradhan, N., and Zhong, H. (2018). From Large Scale Synthesis to Lighting Device Applications of Ternary I–III–VI Semiconductor Nanocrystals: The Inspiring Greener Material Emitters. *The Journal of Physical Chemistry Letters*, 9(2), 435–445.
- Cho, J. S., Lee, S. M., Jung, K. Y., and Kang, Y. C. (2014). Large-scale production of fine-sized $Zn_2SiO_4:Mn$ phosphor microspheres with a dense structure and good photoluminescence properties by a spray-drying process. *RSC Advances*, 4(82), 43606–43611.
- Coats, A. W., and Redfern, J. P. (1963). Thermogravimetric analysis. A review. *Analyst*, 88(1053), 906–924.
- Coe-Sullivan, S. (2009). Optoelectronics: Quantum dot developments. *Nature Photonics*, 3(6), 315–316.
- Coppola, V., Boni, M., Gilg, H. A., Balassone, G., and Dejonghe, L. (2008a). The “calamine” nonsulfide Zn–Pb deposits of Belgium: petrographical, mineralogical and geochemical characterization. *Ore Geology Reviews*, 33(2), 187–210.
- Cui, H., Zayat, M., and Levy, D. (2005). Nanoparticle Synthesis of Willemite Doped with Cobalt Ions ($Co_{0.05}Zn_{1.95}SiO_4$) by an Epoxide-Assisted Sol–Gel Method. *Chemistry of Materials*, 17(22), 5562–5566.
- Dai, P., Sun, Y. Q., Bao, Z. W., Zhu, J., and Wu, M. Z. (2017). Optical and adsorption properties of mesoporous $SiO_2/Zn_2SiO_4:Eu^{3+}$ hollow nanospheres. *Micro and Nano Letters*, 12(4), 248–251.
- Damodaran, V., and Ghosh, K. (2018). Size Optimization of InAs/GaAs Quantum Dots for Longer Storage Memory Applications. In *Nanoelectronic Materials and Devices* 9–35. Springer, Singapore.
- Dang, L., Tian, C., Zhao, S., and Lu, Q. (2018). Barium and manganese-doped zinc silicate rods prepared by mesoporous template route and their luminescence property. *Journal of Crystal Growth*, 491, 126–131.

- Dang, L., Zhang, M., Tian, C., Zhao, S., and Lu, Q. (2017). Solid-state reaction route to synthesis of ordered mesoporous β -Zn₂SiO₄:Mn–SiO₂ composites with ultraviolet and yellow emission. *Optical Materials*, 73, 241–246.
- Davis, E. A., and Mott, N.F. (1970). Conduction in non-crystalline systems V. Conductivity, optical absorption and photoconductivity in amorphous semiconductors. *Philosophical Magazine*, 22(179), 0903–0922.
- Dieing, T., and Ibach, W. (2010). Software requirements and data analysis in confocal Raman microscopy. In *Confocal Raman Microscopy*, 61–89. Springer.
- Ding, L., Ning, W., Wang, Q., Shi, D., and Luo, L. (2015). Preparation and characterization of glass–ceramic foams from blast furnace slag and waste glass. *Materials Letters*, 141, 327–329.
- Dinsmore, A. D., Hsu, D. S., Gray, H. F., Qadri, S. B., Tian, Y., and Ratna, B. R. (1999). Mn-doped ZnS nanoparticles as efficient low-voltage cathodoluminescent phosphors. *Applied Physics Letters*, 75(6), 802–804.
- DJačanin, L., Lukić, S. R., Petrović, D. M., Nikolić, M., and Dramičanin, M. D. (2011). Judd–Ofelt analysis of luminescence emission from Zn₂SiO₄:Eu₃₊ nanoparticles obtained by a polymer-assisted sol–gel method. *Physica B: Condensed Matter*, 406(11), 2319–2322.
- Dong, Y., Qiao, T., Kim, D., Parobek, D., Rossi, D., and Son, D. H. (2018). Precise Control of Quantum Confinement in Cesium Lead Halide Perovskite Quantum Dots via Thermodynamic Equilibrium. *Nano Letters*, 18(6), 3716–3722.
- Doroshev, A. M., Olesch, M., Logvinov, V. M., and Malinovsky, I. J. (1983). High-pressure stability of zinc clinopyroxene znsio₃ and the occurrence of a new polytype of zinc orthosilicate Zn₂SiO₄ as a breakdown product. *Neues Jahrbuch Fur Mineralogie–Monatshefte*, (6), 277–288.
- Drexler, K. E., Peterson, C., and Pergamit, G. (1991). Unbounding the future. *William Morrow, New York, USA*.
- Duoduo, M., and Xingren, L. (1998). Crystal structures and phase transition on Gd₂O₃:Eu nanophosphors. *Chinese Journal of Luminescence*, 19(3), 1–3.
- Effendy, N., Wahab, Z. A., Abdul Aziz, S. H., Matori, K. A., Zaid, M. H. M., and Rashid, S. S. A. (2017). Characterization and optical properties of erbium oxide doped ZnO–SLS glass for potential optical and optoelectronic materials. *Materials Express*, 7(1), 59–65.
- El Ghoul, J. (2018). Green and yellow luminescence properties of Willemite Zn₂SiO₄ nanocomposites by sol–gel method. *Journal of Materials Science: Materials in Electronics*, 29(4), 2999–3005.

- El Ghoul, J., Barthou, C., Saadoun, M., and El Mir, L. (2010). Synthesis and optical characterization of $\text{SiO}_2/\text{Zn}_2\text{SiO}_4:\text{Mn}$ nanocomposite. *Physica B: Condensed Matter*, 405(2), 597–601.
- El Ghoul, J., and El Mir, L. (2014). Sol–gel synthesis and luminescence of undoped and Mn-doped zinc orthosilicate phosphor nanocomposites. *Journal of Luminescence*, 148, 82–88.
- El Ghoul, J., Ghiloufi, I., and El Mir, L. (2016). Effect of annealing temperature on the luminescence properties of $\text{Zn}_2\text{SiO}_4:\text{V}$ nanocomposite. *Journal of Luminescence*, 170, 288–292.
- El Ghoul, J., Omri, K., Alyamani, A., Barthou, C., and El Mir, L. (2013). Synthesis and luminescence of $\text{SiO}_2/\text{Zn}_2\text{SiO}_4$ and $\text{SiO}_2/\text{Zn}_2\text{SiO}_4:\text{Mn}$ composite with sol–gel methods. *Journal of Luminescence*, 138, 218–222.
- El Ghoul, J., Omri, K., El Mir, L., Barthou, C., and Alaya, S. (2012). Sol–gel synthesis and luminescent properties of $\text{SiO}_2/\text{Zn}_2\text{SiO}_4$ and $\text{SiO}_2/\text{Zn}_2\text{SiO}_4:\text{V}$ composite materials. *Journal of Luminescence*, 132(9), 2288–2292.
- El Ghoul, J., Omri, K., Gómez-Lopera, S. A., and El Mir, L. (2014). Sol–gel synthesis, structural and luminescence properties of MT-doped $\text{SiO}_2/\text{Zn}_2\text{SiO}_4$ nanocomposites. *Optical Materials*, 36(6), 1034–1039.
- El Mir, L., and Omri, K. (2014). Photoconversion from UV–to–yellow in Mn doped zinc silicate nanophosphor material. *Superlattices and Microstructures*, 75, 89–98.
- El Mir, L., and Omri, K. (2018). Effect of manganese content on the yellow luminescence properties of zinc silicate nanoparticles enriched silica matrix. *Journal of Luminescence*, 203, 336–340.
- El Mir, L., Omri, K., and El Ghoul, J. (2015). Effect of crystallographic phase on green and yellow emissions in Mn-doped zinc silicate nanoparticles incorporated in silica host matrix. *Superlattices and Microstructures*, 85, 180–184.
- Elhadi, S. E., Liu, C., Zhao, Z., Li, K., and Zhao, X. (2018). Structure and optical properties of $\text{ZnO}/\text{Zn}_2\text{SiO}_4$ composite thin films containing Eu^{3+} ions. *Thin Solid Films*, 668, 1–8.
- Engku Ali, E. A. G., Matori, K. A., Saion, E., Sidek, H. A. A., Zaid, M. H. M., and Alibe, I. M. (2017). Effect of reaction time on structural and optical properties of porous SiO_2 nanoparticles. *Digest Journal of Nanomaterials and Biostructure*, 12, 441–447.
- Erol, O., Uyan, I., Hatip, M., Yilmaz, C., Tekinay, A. B., and Guler, M. O. (2017). Recent advances in bioactive 1D and 2D carbon nanomaterials for

- biomedical applications. *Nanomedicine: Nanotechnology, Biology and Medicine*, 14(7), 2433–2454
- Falcony, C., Aguilar-Frutis, M., and García-Hipólito, M. (2018). Spray Pyrolysis Technique; High-K Dielectric Films and Luminescent Materials: A Review. *Micromachines*, 9(8), 414.
- Feldman, C., and O'Hara, M. (1958). Luminescent Phases in Willemite Films. *JOSA*, 48(11), 816–820.
- Feldmann, C., Jüstel, T., Ronda, C. R., and Schmidt, P. J. (2003). Inorganic luminescent materials: 100 years of research and application. *Advanced Functional Materials*, 13(7), 511–516.
- Feynman, R. P. (1960). There's plenty of room at the bottom. *Engineering and Science*, 23(5), 22–36.
- Fonda, G. R. (1940). The Yellow and Red Zinc Silicate Phosphors. *The Journal of Physical Chemistry*, 44(7), 851–861.
- Fritzsche, H. (1971). Optical and electrical energy gaps in amorphous semiconductors. *Journal of Non-Crystalline Solids*, 6(1), 49–71.
- Fu, Z., Yang, B., Li, L., Dong, W., Jia, C., and Wu, W. (2003). An intense ultraviolet photoluminescence in sol-gel ZnO-SiO₂ nanocomposites. *Journal of Physics: Condensed Matter*, 15(17), 2867.
- Fuller, S. B., Wilhelm, E. J., and Jacobson, J. M. (2002). Ink-jet printed nanoparticle microelectromechanical systems. *Journal of Microelectromechanical System*, 11(1), 54–60.
- Gandhi, V., Ganesan, R., Abdulrahman Syedahamed, H. H., and Thaiyan, M. (2014). Effect of cobalt doping on structural, optical, and magnetic properties of ZnO nanoparticles synthesized by coprecipitation method. *The Journal of Physical Chemistry C*, 118(18), 9715–9725.
- Gao, F., Naik, S. P., Sasaki, Y., and Okubo, T. (2006). Preparation and optical property of nanosized ZnO electrochemically deposited in mesoporous silica films. *Thin Solid Films*, 495(1–2), 68–72.
- Gao, X. D., Li, X. M., and Yu, W. D. (2004). Synthesis and optical properties of ZnO nanocluster porous films deposited by modified SILAR method. *Applied Surface Science*, 229(1), 275–281.
- Garakyaraghi, S., and Castellano, F. N. (2018). Nanocrystals for triplet sensitization: Molecular behavior from quantum-confined materials. *ACS Publications*, (57)5, 2351–2359

- Gardiner, D. J. (1989). Introduction to Raman scattering. In *Practical Raman Spectroscopy* 1–12. Springer.
- Gene, S. A., Saion, E., Shaari, A. H., Kamarudin, M. A., Al-Hada, N. M., and Kharazmi, A. (2014). Structural, optical, and magnetic characterization of spinel zinc chromite nanocrystallines synthesised by thermal treatment method. *Journal of Nanomaterials*, 2014(15) 1–7.
- Gharibshahi, L., Saion, E., Gharibshahi, E., Shaari, A. H., and Matori, K. A. (2017a). Influence of Poly (vinylpyrrolidone) concentration on properties of silver nanoparticles manufactured by modified thermal treatment method. *PloS One*, 12(10), e0186094.
- Gharibshahi, L., Saion, E., Gharibshahi, E., Shaari, A. H., and Matori, K. A. (2017b). Structural and optical properties of Ag nanoparticles synthesized by thermal treatment method. *Materials*, 10(4), 1–13.
- Gholinejad, M., Zareh, F., and Nájera, C. (2018). Nitro group reduction and Suzuki reaction catalysed by palladium supported on magnetic nanoparticles modified with carbon quantum dots generated from glycerol and urea. *Applied Organometallic Chemistry*, 32(1), e3984.
- Giri, N., Natarajan, R. K., Gunasekaran, S., and Shreemathi, S. (2011). ¹³C NMR and FTIR spectroscopic study of blend behavior of PVP and nano silver particles. *Archives of Applied Science Research*, 3(5), 624–30.
- Gnutzmann, U., and Clausecker, K. (1974). Theory of direct optical transitions in an optical indirect semiconductor with a superlattice structure. *Applied Physics*, 3(1), 9–14.
- Goldman, D. E., and Richards, J. R. (1954). Measurement of High-Frequency Sound Velocity in Mammalian Soft Tissues. *The Journal of the Acoustical Society of America*, 26(6), 981–983.
- Goldstein, J. I., Newbury, D. E., Michael, J. R., Ritchie, N. W., Scott, J. H. J., and Joy, D. C. (2017). *Scanning electron microscopy and X-ray microanalysis*. Springer.
- Goodarz Naseri, M., Saion, E. B., and Kamali, A. (2012). An overview on nanocrystalline ZnFe₂O₄, MnFe₂O₄, and CoFe₂O₄ synthesized by a thermal treatment method. *ISRN Nanotechnology*, 2012, 1–11.
- Götz, J., and Masson, C. R. (1970). Trimethylsilyl derivatives for the study of silicate structures. Part I. A direct method of trimethylsilylation. *Journal of the Chemical Society A: Inorganic, Physical, Theoretical*, 0, 2683–2686.
- Graves, P. R., and Gardiner, D. J. (1989). *Practical Raman Spectroscopy*. Springer.

- Grigorie, A. C., Muntean, C., Vlase, T., Locovei, C., and Stefanescu, M. (2017). ZnO–SiO₂ based nanocomposites prepared by a modified sol–gel method. *Materials Chemistry and Physics*, 186, 399–406.
- Gun’Ko, V. M., Bogatyrov, V. M., Oranska, O. I., Borysenko, L. I., Skubiszewska–Zięba, J., Książek, A., and Leboda, R. (2013). Structural features of ZnxOy/nanosilica composites. *Applied Surface Science*, 276, 802–809.
- Guozhong, C. (2004). *Nanostructures and Nanomaterials: synthesis, properties and applications*. World scientific.
- Gupta, D., Meher, S. R., Illyaskutty, N., and Alex, Z. C. (2018). Facile synthesis of Cu₂O and CuO nanoparticles and study of their structural, optical and electronic properties. *Journal of Alloys and Compounds*, 743, 737–745.
- Hafeez, M., Ali, A., Manzoor, S., and Bhatti, A. S. (2014). Anomalous optical and magnetic behavior of multi–phase Mn doped Zn₂SiO₄ nanowires: a new class of dilute magnetic semiconductors. *Nanoscale*, 6(24), 14845–14855.
- Hao, Y., and Wang, Y. (2007). Luminescent properties of Zn₂SiO₄:Mn²⁺ phosphor under UV, VUV and CR excitation. *Journal of Luminescence*, 122, 1006–1008.
- Harris, D. C. (2010). *Quantitative chemical analysis*. Macmillan, London United Kingdom.
- Harrison, D. E. (1960). Relation of Some Surface Chemical Properties of Zinc Silicate Phosphor to its Behavior in Fluorescent Lamps. *Journal of the Electrochemical Society*, 107(3), 210–217.
- Hayes, G. R., and Deveaud, B. (2002). Is luminescence from quantum wells due to excitons? *Physica Status Solidi (A)*, 190(3), 637–640.
- Hernandez–Calderon, I. (2018). Optical properties and electronic structure of wide band gap II–VI semiconductors. In *II–VI Semiconductor Materials and their Applications* 113–170 Routledge.
- Hitzman, M. W., Reynolds, N. A., Sangster, D. F., Allen, C. R., and Carman, C. E. (2003). Classification, genesis, and exploration guides for nonsulfide zinc deposits. *Economic Geology*, 98(4), 685–714.
- Hong, J.–H., Wang, Y.–F., He, G., and Wang, J.–X. (2010). The effect of calcination temperature on the photoluminescence from sol–gel derived amorphous ZnO/silica composites. *Journal of Non–Crystalline Solids*, 356(50–51), 2778–2780.
- Horikoshi, S., and Serpone, N. (2013). Introduction to nanoparticles. *Microwaves in Nanoparticle Synthesis: Fundamentals and Applications*, 1–24.

- Hybertsen, M. S., and Louie, S. G. (1985). First-principles theory of quasiparticles: calculation of band gaps in semiconductors and insulators. *Physical Review Letters*, 55(13), 1418.
- Ider, M., Abderrafi, K., Eddahbi, A., Ouaskit, S., and Kassiba, A. (2017). Silver metallic nanoparticles with surface plasmon resonance: Synthesis and characterizations. *Journal of Cluster Science*, 28(3), 1051–1069.
- Iijima, S. (1991). Helical microtubules of graphitic carbon. *Nature* 354, 56–58.
- Jacob, S., Hanumantharayappa, C., and Nagabhushana, B. M. (2018). Precursors effect: Photo conversion from UV to green/yellow in willemite nano phosphors. *Optik*, 173, 88–96.
- Jal, P. K., Sudarshan, M., Saha, A., Patel, S., and Mishra, B. K. (2004). Synthesis and characterization of nanosilica prepared by precipitation method. *Colloids and Surfaces A: Physicochemical and Engineering Aspects*, 240(1–3), 173–178.
- Jenkins, A., and Stephens, P. W. (1991). X-ray diffraction inspection system, U.S. Patent No. 5,007,072. Washington, DC: U.S. Patent and Trademark Office.
- Jiang, Y., Chen, J., Xie, Z., and Zheng, L. (2010). Syntheses and optical properties of α -and β -Zn₂SiO₄:Mn nanoparticles by solvothermal method in ethylene glycol–water system. *Materials Chemistry and Physics*, 120(2–3), 313–318.
- Jing, Y., Ma, Y., Li, Y., and Heine, T. (2017). GeP3: A small indirect band gap 2D crystal with high carrier mobility and strong interlayer quantum confinement. *Nano Letters*, 17(3), 1833–1838.
- Jung, K. Y., and Han, K. H. (2005). Densification and photoluminescence improvement of Y₂O₃ phosphor particles prepared by spray pyrolysis. *Electrochemical and Solid-State Letters*, 8(2), H17–H20.
- Kairdolf, B. A., Qian, X., and Nie, S. (2017). Bioconjugated nanoparticles for biosensing, in vivo imaging, and medical diagnostics. *Analytical Chemistry*, 89(2), 1015–1031.
- Kamari, H. M., Al-Hada, N. M., Saion, E., Shaari, A. H., Talib, Z. A., Flaifel, M. H., and Ahmed, A. A. A. (2017). Calcined solution-based PVP influence on ZnO semiconductor nanoparticle properties. *Crystals*, 7(2), 1–14.
- Kang, Y. C., Lim, M. A., Park, H. D., and Han, M. (2003). Ba²⁺ co-doped Zn₂SiO₄:Mn phosphor particles prepared by spray pyrolysis process. *Journal of the Electrochemical Society*, 150(1), H7–H11.
- Kang, Y. C., and Park, H. D. (2003). Brightness and decay time of Zn₂SiO₄:Mn phosphor particles with spherical shape and fine size. *Applied Physics A*, 77(3–4), 529–532.

- Kang, Y. C., Park, H. D., and Lim, M. (2001). Zn₂SiO₄:Mn Phosphor Particles Prepared by Spray Pyrolysis Process. *Journal of Information Display*, 2(4), 57–62.
- Kang, Z., Jiao, K., Cheng, J., Peng, R., Jiao, S., and Hu, Z. (2018). A novel three-dimensional carbonized PANI1600@ CNTs network for enhanced enzymatic biofuel cell. *Biosensors and Bioelectronics*, 101, 60–65.
- Karazhanov, S. Z., Ravindran, P., Fjellvåg, H., and Svensson, B. G. (2009). Electronic structure and optical properties of ZnSiO₃ and Zn₂SiO₄. *Journal of Applied Physics*, 106(12), 1–8.
- Karoui, R. (2018). Spectroscopic Technique: Fluorescence and Ultraviolet–Visible (UV–Vis) Spectroscopies. In *Modern techniques for food authentication* pp. 219–252. Academic Press.
- Katsuki T, and Yoshiyasu S. (1960). Studies on Interaction between Solids (II) Transfer of Zinc Oxide on Crystal Surface. *Journal of Japanese Chemistry*, 81(9), 1399–1401.
- Keiteb, Aysar S., Saion, E., Zakaria, A., and Soltani, N. (2016a). Structural and optical properties of zirconia nanoparticles by thermal treatment synthesis. *Journal of Nanomaterials*, 2016, 1–6.
- Keiteb, Aysar Sabah, Saion, E., Zakaria, A., Soltani, N., and Abdullahi, N. (2016b). A modified thermal treatment method for the up-scalable synthesis of size-controlled nanocrystalline titania. *Applied Sciences*, 6(10), 295.
- Kim, D., El-Shall, H., Dennis, D., and Morey, T. (2005). Interaction of PLGA nanoparticles with human blood constituents. *Colloids and Surfaces B: Biointerfaces*, 40(2), 83–91.
- Kim, Y. T., Han, J. H., Hong, B. H., and Kwon, Y. U. (2010). Electrochemical synthesis of CdSe quantum-dot arrays on a graphene basal plane using mesoporous silica thin-film templates. *Advanced Materials*, 22(4), 515–518.
- King, E. G. (1951). Heats of Formation of Crystalline Calcium Orthosilicate, Tricalcium Silicate and Zinc Orthosilicate1. *Journal of the American Chemical Society*, 73(2), 656–658.
- Klaska, K.–H., Eck, J. C., and Pohl, D. (1978). New investigation of willemite. *Acta Crystallographica Section B: Structural Crystallography and Crystal Chemistry*, 34(11), 3324–3325.
- Klimov, V. I., Mikhailovsky, A. A., Xu, S., Malko, A., Hollingsworth, J. A., Leatherdale, a C., Eisler, H.J., and Bawendi, M. G. (2000). Optical gain and stimulated emission in nanocrystal quantum dots. *Science*, 290(5490), 314–317.

- Kobosko, S. M., and Kamat, P. V. (2018). Indium–Rich AgInS₂–ZnS Quantum Dots–Ag: Zn Dependent Photophysics and Photovoltaics. *The Journal of Physical Chemistry C*, 122(26), 14336–14344.
- Kodaira, K., Ito, S., and Matsushita, T. (1975). Hydrothermal growth of willemite single crystals in acidic solutions. *Journal of Crystal Growth*, 29(1), 123–124.
- Kolekar, T. V., Bandgar, S. S., Yadav, H. M., Shirguppikar, S. S., Shinde, M. A., and Magalad, V. T. (2017). Studies on Cancer Cell Cytotoxicity, Antimicrobial Activity of Sol–Gel Synthesized Willemite for Biomedical Applications. *Current Nanoscience*, 13(5), 469–475.
- Kracker, M., Thieme, C., Häßler, J., and Rüssel, C. (2016). Sol–gel powder synthesis and preparation of ceramics with high–and low–temperature polymorphs of Ba_xSr_{1-x}Zn₂Si₂O₇ ($x = 1$ and 0.5): A novel approach to obtain zero thermal expansion. *Journal of the European Ceramic Society*, 36(8), 2097–2107.
- Kumar, K. S., Choudhary, N., Jung, Y., and Thomas, J. (2018). Recent advances in two–dimensional nanomaterials for supercapacitor electrode applications. *ACS Energy Letters*, 3(2), 482–495.
- Kumari, P., Dwivedi, Y., and Bahadur, A. (2018). Analysis of bright red–orange emitting Mn²⁺:ZnAl₂O₄ spinel nanophosphor. *Optik–International Journal for Light and Electron Optics*, 154, 126–132.
- Larkin, P. (2017). *Infrared and Raman spectroscopy: principles and spectral interpretation*. Elsevier.
- Lee, C. H., Kang, Y. C., Jung, K. Y., and Choi, J. G. (2005). Phosphor layer formed from the Zn₂SiO₄:Mn phosphor particles with spherical shape and fine size. *Materials Science and Engineering: B*, 117(2), 210–215.
- Lee, C. S., Matori, K. A., Ab Aziz, S. H., Kamari, H. M., Ismail, I., and Zaid, M. H. M. (2017). Influence of zinc oxide on the physical, structural and optical band gap of zinc silicate glass system from waste rice husk ash. *Optik–International Journal for Light and Electron Optics*, 136, 129–135.
- Lee, J. S., Oh, M. H., Kumar, P., Khanna, A., Singh, R. K., and Ranade, M. B. (2011). Mn–Doped Zn₂SiO₄ phosphors synthesis using flame spray pyrolysis. *Journal of Thermal Spray Technology*, 20(5), 1001–1008.
- Lenggoro, I. W., Iskandar, F., Mizushima, H., Xia, B., Okuyama, K., and Kijima, N. (2000). One–step synthesis for Zn₂SiO₄:Mn particles 0.3–1.3 μm in size with spherical morphology and non–aggregation. *Japanese Journal of Applied Physics*, 39(10B), L1051–L1051.
- Leverenz, H. W. An introduction to luminescence of solids. 1950. Wiley and Sons, Inc. Pages, 333, 53–54.

- Leverenz, H. W. (1949). Luminescent solids (phosphors). *Science*, 109(2826), 183–195.
- Leverenz, H. W., and Seitz, F. (1939). Luminescent materials. *Journal of Applied Physics*, 10(7), 479–493.
- Lewis, I. R., and Edwards, H. (2001). *Handbook of Raman spectroscopy: from the research laboratory to the process line*. CRC Press.
- Li, B., Zhou, J., Zong, R., Fu, M., Li, L., and Li, Q. (2006). Strong suppression and enhancement of photoluminescence in $Zn_2SiO_4:Mn^{2+}$ inverse opal photonic crystals. *Journal of the American Ceramic Society*, 89(7), 2308–2310.
- Li, Q. H., Komarneni, S., and Roy, R. (1995). Control of morphology of Zn_2SiO_4 by hydrothermal preparation. *Journal of Materials Science*, 30(9), 2358–2363.
- Li, X., Zhao, Y. B., Fan, F., Levina, L., Liu, M., Quintero-Bermudez, R., Gong, X., Quan, L.N., Fan, J., Yang, Z. and Hoogland, S. (2018). Bright colloidal quantum dot light-emitting diodes enabled by efficient chlorination. *Nature Photonics*, 12(3), 159.
- Lim, S.–G., Kriventsov, S., Jackson, T. N., Haeni, J. H., Schlom, D. G., Balbashov, A. M., Uecker, R., Reiche, P., Freeouf, J.L. and Lucovsky, G. (2002). Dielectric functions and optical bandgaps of high-K dielectrics for metal–oxide–semiconductor field–effect transistors by far ultraviolet spectroscopic ellipsometry. *Journal of Applied Physics*, 91(7), 4500–4505.
- Lin, C., Wang, J., Zhao, X., Zhu, E., Long, N., and Rüssel, C. (2018). Competitive crystallization of β - Zn_2SiO_4 and ZnO in an aluminosilicate glass. *Ceramics International*, 44(6), 7209–7213.
- Lin, C. C., and Shen, P. (1994). Sol–gel synthesis of zinc orthosilicate. *Journal of Non–Crystalline Solids*, 171(3), 281–289.
- Lin, J., Zhang, C., Yan, Z., Zhu, Y., Peng, Z., Hauge, R.H., Natelson, D. and Tour, J.M. (2012). 3-dimensional graphene carbon nanotube carpet-based microsupercapacitors with high electrochemical performance. *Nano Letters*, 13(1), 72–78.
- Lin–Vien, D., Colthup, N. B., Fateley, W. G., and Grasselli, J. G. (1991). *The handbook of infrared and Raman characteristic frequencies of organic molecules*. Academic Press: New York, NY, USA.
- Liu, L., Zhang, C., Gu, Y., Yang, L., Cheng, Y., Jiang, P., and Wang, J. (2018). A facile method for the preparation of quantum dots–DNA nanoprobe. *Nanomedicine: Nanotechnology, Biology and Medicine*, 14(5), 1847.
- Liu, P., Jin, L. N., Jin, C., Zhang, J. N., and Bian, S.W. (2018). Synthesis of hierarchically porous silicate–1 and ZSM–5 by hydrothermal transformation

- of SiO_2 colloid crystal/carbon composites. *Microporous and Mesoporous Materials*, 262, 217–226.
- Loganathan, S., Valapa, R. B., Mishra, R. K., Pugazhenthi, G., and Thomas, S. (2017). Thermogravimetric Analysis for Characterization of Nanomaterials. In *Thermal and Rheological Measurement Techniques for Nanomaterials Characterization* 67–108. Elsevier.
- Lojpur, V., Nikolić, M. G., Jovanović, D., Medić, M., Antić, Ž., and Dramićanin, M. D. (2013). Luminescence thermometry with $\text{Zn}_2\text{SiO}_4:\text{Mn}^{2+}$ powder. *Applied Physics Letters*, 103(14), 141912.
- Loría-Bastarrachea, M. I., Herrera-Kao, W., Cauich-Rodríguez, J. V., Cervantes-Uc, J. M., Vázquez-Torres, H., and Ávila-Ortega, A. (2010). A TG/FTIR study on the thermal degradation of poly (vinyl pyrrolidone). *Journal of Thermal Analysis and Calorimetry*, 104(2), 737–742.
- Lukić, S. R., Petrović, D. M., Dramićanin, M. D., Mitrić, M., and Đačanin, L. (2008a). Optical and structural properties of $\text{Zn}_2\text{SiO}_4:\text{Mn}^{2+}$ green phosphor nanoparticles obtained by a polymer-assisted sol-gel method. *Scripta Materialia*, 58(8), 655–658.
- Luo, Y., Geng, S., Dube, L., and Zhao, J. (2018). Tuning the Valency of Heterogeneous Au–Silica Nanostructure via Controlled Ostwald Ripening Process. *The Journal of Physical Chemistry C*, 122(31), 18077–18085.
- Lux, F., Tillement, O., Saint Jean, M., Mowat, P., Perriat, P., Roux, S., and Mignot, A. (2018). Ultrafine nanoparticles comprising a functionalized polyorganosiloxane matrix and including metal complexes; method for obtaining same and uses thereof in medical imaging and/or therapy, U.S. Patent Application No. 15/677,167.
- Lyell, C. (1855). *A manual of elementary geology*. John Murray, London United Kingdom.
- Lyman, C. E., Newbury, D. E., Goldstein, J., Williams, D.B., Romig Jr, A.D., Armstrong, J., Echlin, P., Fiori, C., Joy, D.C., Lifshin, E. and Peters, K.R. (2012). *Scanning electron microscopy, X-ray microanalysis, and analytical electron microscopy: a laboratory workbook*. Springer Science and Business Media.
- Ma, Q., Yu, Y., Sindoro, M., Fane, A. G., Wang, R., and Zhang, H. (2017). Carbon-Based Functional Materials Derived from Waste for Water Remediation and Energy Storage. *Advanced Materials*, 29(13), 1605361.
- Madhuri, V., Kumar, J. S., Rao, M. S., and Cole, S. (2015). Investigations on spectral features of tungsten ions in sodium lead alumino borate glass system. *Journal of Physics and Chemistry of Solids*, 78, 70–77.

- Mahmud, M.A., Elumalai, N.K., Upama, M.B., Wang, D., Puthen-Veettil, B., Haque, F., Wright, M., Xu, C., Pivrikas, A. and Uddin, A. (2017). Controlled Ostwald ripening mediated grain growth for smooth perovskite morphology and enhanced device performance. *Solar Energy Materials and Solar Cells*, 167, 87–101.
- Mallick, A., Mahapatra, A. S., Mitra, A., Greneche, J. M., Ningthoujam, R. S., and Chakrabarti, P. K. (2018). Magnetic properties and bio-medical applications in hyperthermia of lithium zinc ferrite nanoparticles integrated with reduced graphene oxide. *Journal of Applied Physics*, 123(5), 1–9.
- Mallur, S. B., Czarnecki, T., Adhikari, A., and Babu, P. K. (2015). Compositional dependence of optical band gap and refractive index in lead and bismuth borate glasses. *Materials Research Bulletin*, 68, 27–34.
- Mandrycky, C., Wang, Z., Kim, K., and Kim, D.-H. (2016). 3D bioprinting for engineering complex tissues. *Biotechnology Advances*, 34(4), 422–434.
- Markham, N. L. (1960). The willemite–hemimorphite relationship. *Economic Geology*, 55(4), 844–847.
- Marumo, Fum., and Syono, Y. (1971). The crystal structure of Zn_2SiO_4 –II, a high-pressure phase of willemite. *Acta Crystallographica Section B*, 27(10), 1868–1870.
- Masjedi–Arani, M., and Salavati–Niasari, M. (2016). A simple sonochemical approach for synthesis and characterization of Zn_2SiO_4 nanostructures. *Ultrasonics Sonochemistry*, 29, 226–235.
- Mbule, P. S., Mothudi, B. M., and Dhlamini, M. S. (2017). Mn^{2+} – Eu^{3+} – Dy^{3+} doped and co-doped Zn_2SiO_4 nanophosphors: Study of the structure, photoluminescence and surface properties. *Journal of Luminescence*, 192, 853–859.
- McHugh, K.J., Jing, L., Behrens, A.M., Jayawardena, S., Tang, W., Gao, M., Langer, R. and Jaklenec, A. (2018). Biocompatible Semiconductor Quantum Dots as Cancer Imaging Agents. *Advanced Materials*, 30(18), 1706356.
- McNaught, A. D., and McNaught, A. D. (1997). *Compendium of chemical terminology* (Vol. 1669). Blackwell Science Oxford.
- Meier, U., and Pettenkofer, C. (2005). Morphology of the Si–ZnO interface. *Applied Surface Science*, 252(4), 1139–1146.
- Minami, T. (2003). Oxide thin-film electroluminescent devices and materials. *Solid-State Electronics*, 47(12), 2237–2243.
- Mishra, K. C., Johnson, K. H., DeBoer, B. G., Berkowitz, J. K., Olsen, J., and Dale, E. A. (1991). First principles investigation of electronic structure and

- associated properties of zinc orthosilicate phosphors. *Journal of Luminescence*, 47(5), 197–206.
- Mody, H. M., Kannan, S., Bajaj, H. C., Manu, V., and Jasra, R. V. (2008). A simple room temperature synthesis of MCM-41 with enhanced thermal and hydrothermal stability. *Journal of Porous Materials*, 15(5), 571–579.
- Mohamed, N., Hassan, J., Matori, K. A., Wahab, Z. A., Ismail, Z. M. M., Baharuddin, N. F., and Rashid, S. S. A. (2017). Influence of Pr doping on the thermal, structural and optical properties of novel SLS-ZnO glasses for red phosphor. *Results in Physics*, 7, 1202–1206.
- Moore, M. N. (2006). Do nanoparticles present ecotoxicological risks for the health of the aquatic environment? *Environment International*, 32(8), 967–976.
- Moradlou, O., Rabiei, Z., Banazadeh, A., Warzywoda, J., and Zirak, M. (2018). Carbon quantum dots as nano-scaffolds for α -Fe₂O₃ growth: Preparation of Ti/CQD@ α -Fe₂O₃ photoanode for water splitting under visible light irradiation. *Applied Catalysis B: Environmental*, 227, 178–189.
- Morimo, R., and Matae, K. (1989). Preparation of Zn₂SiO₄:Mn phosphors by alkoxide method. *Materials Research Bulletin*, 24(2), 175–179.
- Morimo, R., Mochinaga, R., and Nakamura, K. (1994). Preparation and characterization of a manganese activated zinc silicate phosphor by fume pyrolysis of an alkoxide solution [Zn₂SiO₄:Mn]. *Materials Research Bulletin*, 29(7), 751–757.
- Mott, N. F., and Davis, E. A. (1971). *Electronic process in non-crystalline materials*. Oxford University Press.
- Murphy, A. B. (2007). Band-gap determination from diffuse reflectance measurements of semiconductor films, and application to photoelectrochemical water-splitting. *Solar Energy Materials and Solar Cells*, 91(14), 1326–1337.
- Nagamine, G., Rocha, J. O., Bonato, L. G., Nogueira, A. F., Cruz, C. B., and Padilha, L. A. (2018). Size Dependent Ultra-low Upconverted Lasing Threshold in CsPbBr₃ Perovskites Quantum Dots. In *Conference on Lasers and Electro-Optics: Applications and Technology* JTU2A–114
- Nakamura, N., Kim, J., and Hosono, H. (2018). Material Design of Transparent Oxide Semiconductors for Organic Electronics: Why Do Zinc Silicate Thin Films Have Exceptional Properties? *Advanced Electronic Materials*, 4(2), 1700352.
- Nam, S .H., Kim, M. H., Lee, J. Y., Lee, S. D., and Boo, J. H. (2010). Spray pyrolysis of manganese doped zinc silicate phosphor particles. *Functional Materials Letters*, 3(02), 97–100.

- Naseri, M. G., Ara, M. H. M., Saion, E. B., and Shaari, A. H. (2014). Superparamagnetic magnesium ferrite nanoparticles fabricated by a simple, thermal–treatment method. *Journal of Magnetism and Magnetic Materials*, 350, 141–147.
- Naseri, M. G., Kamari, H. M., Dehzangi, A., Kamalianfar, A., and Saion, E. B. (2015). Fabrication of a novel chromium–iron oxide ($\text{Cr}_2\text{Fe}_6\text{O}_{12}$) nanoparticles by thermal treatment method. *Journal of Magnetism and Magnetic Materials*, 389, 113–119.
- Naseri, M. G., Saion, E. B., Ahangar, H. A., Hashim, M., and Shaari, A. H. (2011). Simple preparation and characterization of nickel ferrite nanocrystals by a thermal treatment method. *Powder Technology*, 212(1), 80–88.
- Naseri, M. G., Saion, E. B., Ahangar, H. A., and Shaari, A. H. (2013). Fabrication, characterization, and magnetic properties of copper ferrite nanoparticles prepared by a simple, thermal–treatment method. *Materials Research Bulletin*, 48(4), 1439–1446.
- Nashimoto, K., Nakamura, S., and Mariyama, H. (1995). Synthesis and photoluminescence of ZnO nanophosphors. *Japanese Journal of Applied Physics*, 43, 5091.
- Nazarov, M. V., Kang, J. H., Jeon, D. Y., Popovici, E.J., Muresan, L., and Tsukerblat, B. S. (2005). Lattice parameter and luminescence properties of europium activated yttrium oxide. *Solid State Communications*, 133(3), 183–186.
- Ng, S., Kuberský, P., Krbal, M., Prikryl, J., Gärtnerová, V., Moravcová, D., Sopha, H., Zazpe, R., Yam, F.K., Jäger, A. and Hromádko, L. (2018). ZnO Coated Anodic 1D TiO₂ Nanotube Layers: Efficient Photo–Electrochemical and Gas Sensing Heterojunction. *Advanced Engineering Materials*, 20(2), 1700589.
- Nguyen, N. H., Lim, J. B., Nahm, S., Paik, J. H., and Kim, J. H. (2007). Effect of Zn/Si ratio on the microstructural and microwave dielectric properties of Zn₂SiO₄ ceramics. *Journal of the American Ceramic Society*, 90(10), 3127–3130.
- Omar, N. A. S., Fen, Y. W., and Matori, K. A. (2016). Photoluminescence properties of Eu³⁺–doped low cost zinc silicate based glass ceramics. *Optik–International Journal for Light and Electron Optics*, 127(8), 3727–3729.
- Omar, N. A. S., Fen, Y. W., and Matori, K. A. (2017). Europium doped low cost Zn₂SiO₄ based glass ceramics: a study on fabrication, structural, energy band gap and luminescence properties. *Materials Science in Semiconductor Processing*, 61, 27–34.

- Omar, N. A. S., Fen, Y. W., Matori, K. A., Zaid, M. H. M., and Samsudin, N. F. (2016). Structural and optical properties of Eu³⁺ activated low cost zinc soda lime silica glasses. *Results in Physics*, 6, 640–644.
- Omri, K., Alyamani, A., and El Mir, L. (2018). Photoluminescence and cathodoluminescence of Mn doped zinc silicate nanophosphors for green and yellow field emissions displays. *Applied Physics A*, 124(2), 215.
- Omri, K., El Ghoul, J., Alyamani, A., Barthou, C., and El Mir, L. (2013). Luminescence properties of green emission of SiO₂/Zn₂SiO₄:Mn nanocomposite prepared by sol-gel method. *Physica E: Low-Dimensional Systems and Nanostructures*, 53, 48–54.
- Omri, K., and El Mir, L. (2016). In-situ sol-gel synthesis of luminescent Mn²⁺-doped zinc silicate nanophosphor. *Journal of Materials Science: Materials in Electronics*, 27(9), 9476–9482.
- Omri, K., Lemine, O. M., and El Mir, L. (2017). Mn doped zinc silicate nanophosphor with bifunctionality of green-yellow emission and magnetic properties. *Ceramics International*, 43(8), 6585–6591.
- Onufrieva, T. A., Krasnenko, T. I., Zaitseva, N. A., Samigullina, R. F., Enyashin, A. N., Baklanova, I. V., and Tyutyunnik, A. P. (2018a). Concentration growth of luminescence intensity of phosphor Zn_{2-2x}Mn_{2x}SiO₄ ($x \leq 0.13$): Crystal-chemical and quantum-mechanical justification. *Materials Research Bulletin*, 97, 182–188.
- Palache, C. (1935). *The minerals of Franklin and Sterling Hill, Sussex County, New Jersey*. US Government Printing Office.
- Pankratova, G., Pankratov, D., Di Bari, C., Goñi-Urtiaga, A., Toscano, M.D., Chi, Q., Pita, M., Gorton, L. and De Lacey, A.L. (2018). Three-Dimensional Graphene Matrix-Supported and Thylakoid Membrane-Based High-Performance Bioelectrochemical Solar Cell. *ACS Applied Energy Materials*, 1(2), 319–323.
- Parhi, P., and Manivannan, V. (2009). Novel microwave initiated synthesis of Zn₂SiO₄ and MCrO₄ (M= Ca, Sr, Ba, Pb). *Journal of Alloys and Compounds*, 469(1–2), 558–564.
- Park, K. W., Lim, H. S., Park, S. W., Deressa, G., and Kim, J. S. (2015). Strong blue absorption of green Zn₂SiO₄:Mn²⁺ phosphor by doping heavy Mn²⁺ concentrations. *Chemical Physics Letters*, 636, 141–145.
- Patra, A., Baker, G. A., and Baker, S. N. (2005). Effects of dopant concentration and annealing temperature on the phosphorescence from Zn₂SiO₄:Mn²⁺ nanocrystals. *Journal of Luminescence*, 111(1–2), 105–111.

- Pearton, S. J., Norton, D. P., Ip, K., Heo, Y. W., and Steiner, T. (2005). Recent progress in processing and properties of ZnO. *Progress in Materials Science*, 50(3), 293–340.
- Peng, L., Fang, Z., Zhu, Y., Yan, C., and Yu, G. (2018). Holey 2D Nanomaterials for Electrochemical Energy Storage. *Advanced Energy Materials*, 8(9), 1702179.
- Peniche, C., Zaldívar, D., Pazos, M., Páz, S., Bulay, A., and Román, J. S. (1993). Study of the thermal degradation of poly (N-vinyl-2-pyrrolidone) by thermogravimetry-FTIR. *Journal of Applied Polymer Science*, 50(3), 485–493.
- Petrovykh, K. A., Rempel, A. A., Kortov, V. S., and Buntov, E. A. (2015). Sol-gel synthesis and photoluminescence of Zn_2SiO_4 :Mn nanoparticles. *Inorganic Materials*, 51(2), 152–157.
- Pfeiffer, H. G., and Fonda, G. R. (1952). The zinc silicate phosphors fluorescing in the yellow and red. *Journal of the Electrochemical Society*, 99(4), 140–143.
- Pholnak, C., Sirisathitkul, C., Suwanboon, S., and Harding, D. J. (2014). Effects of precursor concentration and reaction time on sonochemically synthesized ZnO nanoparticles. *Materials Research*, 17(2), 405–411.
- Podbršček, P., Dražić, G., Anžlovar, A., and Orel, Z. C. (2011). The preparation of zinc silicate/ZnO particles and their use as an efficient UV absorber. *Materials Research Bulletin*, 46(11), 2105–2111.
- Pokropivny, V. V., and Skorokhod, V. V. (2007). Classification of nanostructures by dimensionality and concept of surface forms engineering in nanomaterial science. *Materials Science and Engineering: C*, 27(5–8), 990–993.
- Polacco, G., Cascone, M. G., Petarca, L., and Peretti, A. (2000). Thermal behaviour of poly (methacrylic acid)/poly (N-vinyl-2-pyrrolidone) complexes. *European Polymer Journal*, 36(12), 2541–2544.
- Pozas, R., Orera, V. M., and Ocana, M. (2005). Hydrothermal synthesis of Co-doped willemite powders with controlled particle size and shape. *Journal of the European Ceramic Society*, 25(13), 3165–3172.
- Qiao, Z., Yan, T., Zhang, X., Zhu, C., Li, W., and Huang, B. (2018). Low-temperature hydrothermal synthesis of Zn_2SiO_4 nanostructures and the novel photocatalytic application in wastewater treatment. *Catalysis Communications*, 106, 78–81.
- Ramakrishna, P. V., Murthy, D., and Sastry, D. L. (2014). Synthesis, structural and luminescence properties of Ti co-doped ZnO/Zn_2SiO_4 : Mn^{2+} composite phosphor. *Ceramics International*, 40(3), 4889–4895.

- Ramakrishna, P. V., Murthy, D., Sastry, D. L., and Samatha, K. (2014). Synthesis, structural and luminescence properties of Mn doped ZnO/Zn₂SiO₄ composite microphosphor. *Spectrochimica Acta Part A: Molecular and Biomolecular Spectroscopy*, 129, 274–279.
- Randall, J. T., and Wilkins, M. H. F. (1945). The phosphorescence of various solids. *Proceedings of the Royal Society of London. A*, 184(999), 347–364.
- Rasdi, N. M., Fen, Y. W., and Omar, N. A. S. (2017). Photoluminescence studies of cobalt (II) doped zinc silicate nanophosphors prepared via sol–gel method. *Optik–International Journal for Light and Electron Optics*, 149, 409–415.
- Rasdi, N. M., Fen, Y. W., Omar, N. A. S., and Zaid, M. H. M. (2017). Effects of cobalt doping on structural, morphological, and optical properties of Zn₂SiO₄ nanophosphors prepared by sol–gel method. *Results in Physics*, 7, 3820–3825.
- Reynaud, L., Brouca–Cabarrecq, C., Mosset, A., and Ahamdane, H. (1996). A new solution route to silicates. Part 3: Aqueous sol–gel synthesis of willemite and potassium antimony silicate. *Materials Research Bulletin*, 31(9), 1133–1139.
- Ringwood, A. E., and Major, A. (1967). High pressure transformations in zinc germanates and silicates. *Nature*, 215(5108), 1367–1368.
- Rivera–Enríquez, C. E., Fernández–Osorio, A., and Chávez–Fernández, J. (2016). Luminescence properties of α– and β–Zn₂SiO₄:Mn nanoparticles prepared by a co–precipitation method. *Journal of Alloys and Compounds*, 688, 775–782.
- Romanov, S. G., Fokin, A. V., and De La Rue, R. M. (2000). Eu³⁺ emission in an anisotropic photonic band gap environment. *Applied Physics Letters*, 76(13), 1656–1658.
- Ronda, C. R. (1997). Recent achievements in research on phosphors for lamps and displays. *Journal of Luminescence*, 72, 49–54.
- Rooksby, H. P., and McKeag, A. H. (1941). The yellow fluorescent form of zinc silicate. *Transactions of the Faraday Society*, 37, 308–311.
- Roy, A., Polarz, S., Rabe, S., Rellinghaus, B., Zähres, H., Kruis, F. E., and Driess, M. (2004). First Preparation of Nanocrystalline Zinc Silicate by Chemical Vapor Synthesis Using an Organometallic Single–Source Precursor. *Chemistry–A European Journal*, 10(6), 1565–1575.
- Roy, D. M., and Mumpton, F. A. (1956). Stability of minerals in the system ZnO–SiO₂–H₂O. *Economic Geology*, 51(5), 432–443.
- Safeera, T. A., and Anila, E. I. (2018). Synthesis and characterization of ZnGa₂O₄:Eu³⁺ nanophosphor by wet chemical method. *Scripta Materialia*, 143, 94–97.

- Sahu, A., Tirosh, S., Hiremath, K. R., Zaban, A., and Dixit, A. (2018). A novel process for sensitization and infiltration of quantum dots in mesoporous metal oxide matrix for efficient solar photovoltaics response. *Solar Energy*, 169, 488–497.
- Salata, O. V. (2004). Applications of nanoparticles in biology and medicine. *Journal of Nanobiotechnology*, 2(1), 3.
- Salem, A., Saion, E., Al-Hada, N. M., Kamari, H. M., Shaari, A. H., Abdullah, C. A. C., and Radiman, S. (2017). Synthesis and characterization of CdSe nanoparticles via thermal treatment technique. *Results in Physics*, 7, 1556–1562.
- Salem, A., Saion, E., Al-Hada, N. M., Kamari, H. M., Shaari, A. H., and Radiman, S. (2017). Simple synthesis of ZnSe nanoparticles by thermal treatment and their characterization. *Results in Physics*, 7, 1175–1180.
- Samigullina, R. F., Tyutyunnik, A. P., Gracheva, I. N., Krasnenko, T. I., Zaitseva, N. A., and Onufrieva, T. A. (2017). Hydrothermal synthesis of α -Zn₂SiO₄:V phosphor, determination of oxidation states and structural localization of vanadium ions. *Materials Research Bulletin*, 87, 27–33.
- Samsudin, N. F., Matori, K. A., Liew, J. Y. C., Wing Fen, Y., Zaid, M., Hafiz, M., and Nadakkavil Alassan, Z. (2015). Investigation on Structural and Optical Properties of Willemite Doped Mn²⁺. *Journal of Spectroscopy*, 2015.
- Sanchez, V. C., Weston, P., Yan, A., Hurt, R. H., and Kane, A. B. (2011). A 3-dimensional in vitro model of epithelioid granulomas induced by high aspect ratio nanomaterials. *Particle and Fibre Toxicology*, 8(1), 17.
- Sartison, M., Engel, L., Kolatschek, S., Olbrich, F., Nawrath, C., Hepp, S., Jetter, M., Michler, P. and Portalupi, S.L. (2018). Deterministic integration and optical characterization of telecom O-band quantum dots embedded into wet-chemically etched Gaussian-shaped microlenses. *Applied Physics Letters*, 113(3), 032103.
- Schappo, H., Gindri, I. M., Cubillos, P. O., Maru, M. M., Salmoria, G. V., and Roesler, C. R. (2018). Scanning Electron Microscopy and Energy-Dispersive X-Ray Spectroscopy as a Valuable Tool to Investigate the Ultra-High-Molecular-Weight Polyethylene Wear Mechanisms and Debris in Hip Implants. *The Journal of Arthroplasty*, 33(1), 258–262.
- Schleede, A., and Gruhl, A. (1923). X-ray observations on fluorescent zinc silicate. *Zeits. f. Elektrochemie*, 29, 411–412.
- Schulz, H. (2018). Spectroscopic technique: Raman spectroscopy. In *Modern Techniques for Food Authentication* 139–191, Elsevier.

- Sekita, M., Iwanaga, K., Hamasuna, T., Mohri, S., Uota, M., Yada, M., and Kijima, T. (2004). Strong Eu emission of annealed Y_2O_3 : Eu nanotube and nano-sized crystals. *Physica Status Solidi (B)*, 241(13), R71–R74.
- Selomulya, R., Ski, S., Pita, K., Kam, C. H., Zhang, Q. Y., and Buddhudu, S. (2003). Luminescence properties of $\text{Zn}_2\text{SiO}_4:\text{Mn}^{2+}$ thin-films by a sol-gel process. *Materials Science and Engineering: B*, 100(2), 136–141.
- Selopal, G.S., Wu, H.P., Lu, J., Chang, Y.C., Wang, M., Vomiero, A., Concina, I. and Diau, E.W.G. (2016). Metal-free organic dyes for TiO_2 and ZnO dye-sensitized solar cells. *Scientific Reports*, 6, 18756.
- Sharma, P., and Bhatti, H. S. (2009). Laser induced down conversion optical characterizations of synthesized $\text{Zn}_{2-x}\text{Mn}_x\text{SiO}_4$ ($0.5 \leq x \leq 5$ mol%) nanophosphors. *Journal of Alloys and Compounds*, 473(1–2), 483–489.
- Shen, T., Li, B., Zheng, K., Pullerits, T., Cao, G., and Tian, J. (2018). Surface Engineering of Quantum Dots for Remarkably High Detectivity Photodetectors. *The Journal of Physical Chemistry Letters*, 9(12), 3285–3294.
- Sheng, L., Liao, T., Kou, L., and Sun, Z. (2017). Single-crystalline ultrathin 2D TiO_2 nanosheets: a bridge towards superior photovoltaic devices. *Materials Today Energy*, 3, 32–39.
- Shevchenko, E. V., Talapin, D. V., Rogach, A. L., Kornowski, A., Haase, M., and Weller, H. (2002). Colloidal synthesis and self-assembly of CoPt_3 nanocrystals. *Journal of the American Chemical Society*, 124(38), 11480–11485.
- Shi, X., Liu, S., Sun, Y., Liang, J., and Chen, Y. (2018). Lowering Internal Friction of 0D–1D–2D Ternary Nanocomposite-Based Strain Sensor by Fullerene to Boost the Sensing Performance. *Advanced Functional Materials*, 28(22), 1800850.
- Shibuki, K., Takesue, M., Aida, T. M., Watanabe, M., Hayashi, H., and Smith Jr, R. L. (2010). Continuous synthesis of $\text{Zn}_2\text{SiO}_4:\text{Mn}^{2+}$ fine particles in supercritical water at temperatures of 400–500° C and pressures of 30–35 MPa. *The Journal of Supercritical Fluids*, 54(2), 266–271.
- Shinde, S. S., Shinde, P. S., Sathe, V. G., Barman, S. R., Bhosale, C. H., and Rajpure, K. Y. (2010). Electron-phonon interaction and size effect study in catalyst based zinc oxide thin films. *Journal of Molecular Structure*, 984(1–3), 186–193.
- Shinde, V. R., Gujar, T. P., and Lokhande, C. D. (2007). LPG sensing properties of ZnO films prepared by spray pyrolysis method: effect of molarity of precursor solution. *Sensors and Actuators B: Chemical*, 120(2), 551–559.

- Shindo, D., and Oikawa, T. (2002). Energy dispersive X-ray spectroscopy. In *Analytical Electron Microscopy for Materials Science* 81–102. Springer.
- Singh, D., Kumar, R., Kumar, A., and Rai, K. N. (2008). Synthesis and characterization of rice husk silica, silica–carbon composite and H₃PO₄ activated silica. *Cerâmica*, 54(330), 203–212.
- Singh, R. G., Singh, F., Mehra, R. M., Kanjilal, D., and Agarwal, V. (2011). Synthesis of nanocrystalline α -Zn₂SiO₄ at ZnO–porous silicon interface: Phase transition study. *Solid State Communications*, 151(9), 701–703.
- Sivaiah, K., Rudramadevi, B. H., and Buddhudu, S. (2010). Structural, thermal and optical properties of Cu²⁺ and Co²⁺: PVP polymer films. *Indian Journal of Pure and Applied Physics*, 48(9), 658–662.
- Skoog, D. A., Holler, F. J., and Crouch, S. R. (2017). Principles of instrumental analysis. Cengage learning.
- Slayter, E. M., and Slayter, H. S. (1992). Light and electron microscopy. Cambridge University Press.
- Smith, A. M., and Nie, S. (2009). Semiconductor nanocrystals: structure, properties, and band gap engineering. *Accounts of Chemical Research*, 43(2), 190–200.
- Smith, R. A. (1978). Semiconductors. Cambridge University Press.
- Song, Y., Liu, T., Yao, B., Li, M., Kou, T., Huang, Z.H., Feng, D.Y., Wang, F., Tong, Y., Liu, X.X. and Li, Y. (2017). Ostwald ripening improves rate capability of high mass loading manganese oxide for supercapacitors. *ACS Energy Letters*, 2(8), 1752–1759.
- Spence, J. C. (1988). *Experimental high-resolution electron microscopy*. Oxford University Press.
- Spence, J.C.H., Kolar, H.R., Hembree, G., Humphreys, C.J., Barnard, J., Datta, R., Koch, C., Ross, F.M. and Justo, J.F. (2006). Imaging dislocation cores—the way forward. *Philosophical Magazine*, 86(29–31), 4781–4796.
- Spencer, L. J. (1929). Fluorescence of minerals in ultra-violet rays. *Mineralogical Society of America*, 14(1), 33–38.
- Stone, V., Nowack, B., Baun, A., van den Brink, N., von der Kammer, F., Dusinska, M., Handy, R., Hankin, S., Hassellöv, M., Joner, E. and Fernandes, T.F. (2010). Nanomaterials for environmental studies: classification, reference material issues, and strategies for physico-chemical characterisation. *Science of the Total Environment*, 408(7), 1745–1754.

- Suárez-Iglesias, O., Collado, S., Oulego, P., and Díaz, M. (2017). Graphene–family nanomaterials in wastewater treatment plants. *Chemical Engineering Journal*, 313, 121–135.
- Sun, H., Zhang, Y., Zhang, J., Sun, X., and Peng, H. (2017). Energy harvesting and storage in 1D devices. *Nature Reviews Materials*, 2(6), 17023.
- Syamimi, N. F., Matori, K. A., Lim, W. F., Abdul Aziz, S., and Mohd Zaid, M. H. (2014). Effect of Sintering Temperature on Structural and Morphological Properties of Europium (III) Oxide Doped Willemite. *Journal of Spectroscopy*, 2014, 1–8.
- Syono, Y., Akimoto, S.I., and Matsui, Y. (1971). High pressure transformations in zinc silicates. *Journal of Solid State Chemistry*, 3(3), 369–380.
- Taghavinia, N., Lerondel, G., Makino, H., Yamamoto, A., Yao, T., Kawazoe, Y., and Goto, T. (2002). Growth of luminescent $Zn_2SiO_4:Mn^{2+}$ particles inside oxidized porous silicon: emergence of yellow luminescence. *Journal of Crystal Growth*, 237, 869–873.
- Takagi, K. (1962). On the Synthesis of Zinc Silicate Phosphor Activated with Manganese by the Solid-state Reaction between Zinc Oxide and Silica. *Journal of the Chemical Society of Japan, Industrial Chemistry Section*, 65(6), 6847–6855.
- Takahashi, S., Imai, Y., Kan, A., Hotta, Y., and Ogawa, H. (2016). Effects of hollow Zn_2SiO_4 particles addition on dielectric properties of isotactic polypropylene–HW composites. *Materials Science and Engineering: B*, 209, 51–55.
- Takesue, M., Hayashi, H., and Smith Jr, R. L. (2009). Thermal and chemical methods for producing zinc silicate (willemite): a review. *Progress in Crystal Growth and Characterization of Materials*, 55(3–4), 98–124.
- Takesue, M., Shimoyama, K., Shibuki, K., Suino, A., Hakuta, Y., Hayashi, H., Ohishi, Y. and Smith Jr, R.L. (2009). Formation of zinc silicate in supercritical water followed with in situ synchrotron radiation X-ray diffraction. *The Journal of Supercritical Fluids*, 49(3), 351–355.
- Takesue, M., Suino, A., Hakuta, Y., Hayashi, H., and Smith Jr, R. L. (2010). Crystallization trigger of Mn-doped zinc silicate in supercritical water via Zn, Mn, Si sources and complexing agent ethylenediamine tetraacetic acid. *Materials Chemistry and Physics*, 121(1–2), 330–334.
- Takesue, M., Suino, A., Shimoyama, K., Hakuta, Y., Hayashi, H., and Smith Jr, R. L. (2008). Formation of α -and β -phase Mn-doped zinc silicate in supercritical water and its luminescence properties at $Si/(Zn^+ Mn)$ ratios from 0.25 to 1.25. *Journal of Crystal Growth*, 310(18), 4185–4189.

- Talapin, D. V., Lee, J. S., Kovalenko, M. V., and Shevchenko, E. V. (2009). Prospects of colloidal nanocrystals for electronic and optoelectronic applications. *Chemical Reviews*, 110(1), 389–458.
- Tammann, G., Westerhold, F., Garre, B., Kordes, E., & Kalsing, H. (1925). Chemical reactions in powdery mixtures of two types of crystals. *Journal of inorganic and general chemistry*, 149(1), 21–98.
- Tarafder, A., Molla, A. R., and Karmakar, B. (2016). Advanced Glass–Ceramic Nanocomposites for Structural, Photonic, and Optoelectronic Applications. In *Glass Nanocomposites* 299–338, Elsevier.
- Tarafder, Anal, Molla, A. R., Mukhopadhyay, S., and Karmakar, B. (2014). Fabrication and enhanced photoluminescence properties of Sm³⁺-doped ZnO–Al₂O₃–B₂O₃–SiO₂ glass derived willemite glass–ceramic nanocomposites. *Optical Materials*, 36(9), 1463–1470.
- Tauc, J., Grigorovici, R., and Vancu, A. (1966). Optical properties and electronic structure of amorphous germanium. *Physica Status Solidi (B)*, 15(2), 627–637.
- Taylor, H. F. W. (1962). The dehydration of hemimorphite. *American Mineralogist: Journal of Earth and Planetary Materials*, 47(7–8), 932–944.
- Taylor, J. (1997). Introduction to error analysis, the study of uncertainties in physical measurements, *University Science Books*, Sausalito U.S.
- Taylor, L. S., Langkilde, F. W., and Zografi, G. (2001). Fourier transform Raman spectroscopic study of the interaction of water vapor with amorphous polymers. *Journal of Pharmaceutical Sciences*, 90(7), 888–901.
- Thanh, N. T. (2018). *Clinical Applications of Magnetic Nanoparticles: From Fabrication to Clinical Applications*. CRC Press.
- Tiwari, J. N., Tiwari, R. N., and Kim, K. S. (2012). Zero-dimensional, one-dimensional, two-dimensional and three-dimensional nanostructured materials for advanced electrochemical energy devices. *Progress in Materials Science*, 57(4), 724–803.
- Toyama, S., Takesue, M., Aida, T. M., Watanabe, M., and Smith Jr, R. L. (2015a). Easy emission–color–control of Mn-doped zinc silicate phosphor by use of pH and supercritical water conditions. *The Journal of Supercritical Fluids*, 98, 65–69.
- Tsao, J.Y., Chowdhury, S., Hollis, M.A., Jena, D., Johnson, N.M., Jones, K.A., Kaplar, R.J., Rajan, S., Van de Walle, C.G., Bellotti, E. and Chua, C.L. (2018). Ultrawide–Bandgap Semiconductors: Research Opportunities and Challenges. *Advanced Electronic Materials*, 4(1), 1600501.

- Uegaito, K., Hosokawa, S., and Inoue, M. (2012). Effect of heat treatments on the luminescence properties of $Zn_2SiO_4:Mn^{2+}$ phosphors prepared by glycothermal methods. *Journal of Luminescence*, 132(1), 64–70.
- Urbach, F. (1953). The long-wavelength edge of photographic sensitivity and of the electronic absorption of solids. *Physical Review*, 92(5), 1324.
- Vaishnavi, T. S., Haridoss, P., and Vijayan, C. (2008). Optical properties of zinc oxide nanocrystals embedded in mesoporous silica. *Materials Letters*, 62(10–11), 1649–1651.
- Van Nieuwenburg, C. J., and Blumendal, H. B. (1931). The pneumatolytic synthesis of silicates. I. *Recueil Des Travaux Chimiques Des Pays-Bas*, 50(2), 129–138.
- Venkataravanappa, M., Nagabhushana, H., Darshan, G. P., Sharma, S. C., Archana, K. V., Basavaraj, R. B., and Prasad, B. D. (2018). Facile ultrasound route for the fabrication of green emitting $Ba_2SiO_4:Eu^{2+}$ nanophosphors for display and dosimetric applications. *Materials Research Bulletin*, 97, 281–292.
- Veremeichik, T. F., Zharikov, E. V., and Subbotin, K. A. (2003). New laser crystals of complex oxides doped with ions of d elements with variable valence and different structural localization. Review. *Crystallography Reports*, 48(6), 974–988.
- Vieira, L. A., Folgueras, M. V., Tomiyama, M., and Prim, S. R. (2018). Rice Husk Ash as a Raw Material to Produce Willemite Pigments. *Materials Science Forum* 912, (44–49).
- Vitkin, V.V., Dymshits, O.S., Polyakov, V.M., Zhilin, A.A., Shemchuk, D.V., Krylov, A.A., Uskov, A.V., Mak, A.A. and Kovalev, A.V. (2017). Pulse-burst Er: glass laser. In *Solid State Lasers XXVI: Technology and Devices* 10082, 1008224.
- Wakefield, G., Holland, E., Dobson, P. J., and Hutchison, J. L. (2001). Luminescence properties of nanocrystalline $Y_2O_3:Eu$. *Advanced Materials*, 13(20), 1557–1560.
- Wan, J., Chen, X., Wang, Z., Mu, L., and Qian, Y. (2005). One-dimensional rice-like Mn-doped Zn_2SiO_4 : Preparation, characterization, luminescent properties and its stability. *Journal of Crystal Growth*, 280(1), 239–243.
- Wan, J., Wang, Z., Chen, X., Mu, L., Yu, W., and Qian, Y. (2006). Controlled synthesis and relationship between luminescent properties and shape/crystal structure of $Zn_2SiO_4:Mn^{2+}$ phosphor. *Journal of Luminescence*, 121(1), 32–38.

- Wang, J., Ge, J., Zhang, H., and Li, Y. (2006). Mn-doped Silicate Micro/Nanowire Bundles on Silicon Wafers: Synthesis and Visible Luminescence. *Small*, 2(2), 257–260.
- Wang, L., Ma, W., Xu, L., Chen, W., Zhu, Y., Xu, C., and Kotov, N. A. (2010). Nanoparticle-based environmental sensors. *Materials Science and Engineering: R: Reports*, 70(3–6), 265–274.
- Wang, W. C., Tian, Y. T., Li, K., Lu, E. Y., Gong, D. S., and Li, X. J. (2013). Capacitive humidity-sensing properties of Zn_2SiO_4 film grown on silicon nanoporous pillar array. *Applied Surface Science*, 273, 372–376.
- Wang, X., Huang, H., Liu, B., Liang, B., Zhang, C., Ji, Q., Chen, D. and Shen, G. (2012). Shape evolution and applications in water purification: the case of CVD-grown Zn_2SiO_4 straw-bundles. *Journal of Materials Chemistry*, 22(12), 5330–5335.
- Wang, Y., Hao, Y., and Yuwen, L. (2006). Synthesis process dependent photoluminescent properties of Zn_2SiO_4 : Mn^{2+} upon VUV region. *Journal of Alloys and Compounds*, 425(1–2), 339–342.
- Wang, Z., and Mi, B. (2017). Environmental applications of 2D molybdenum disulfide (MoS_2) nanosheets. *Environmental Science and Technology*, 51(15), 8229–8244.
- Weber, L., and Oswald, H. R. (1975). Investigation of phase intergrowth morphologies in the system Zn_2SiO_4 – SiO_2 by photo-emission electron microscopy. *Journal of Materials Science*, 10(6), 973–982.
- Wei, Z., Wang, Z., Tait, W.R., Pokhrel, M., Mao, Y., Liu, J., Zhang, L., Wang, W. and Sun, L. (2018). Synthesis of green phosphors from highly active amorphous silica derived from rice husks. *Journal of Materials Science*, 53(3), 1824–1832.
- Weng, Z., Guan, R., and Xiong, Z. (2017). Effects of the ZBS addition on the sintering behavior and microwave dielectric properties of $0.95Zn_2SiO_4$ – $0.05CaTiO_3$ ceramics. *Journal of Alloys and Compounds*, 695, 3517–3521.
- Williamson, J., and Glasser, F. P. (1964). Crystallisation of zinc silicate liquids and glasses. *Physics and Chemistry of Glasses*, 5(1), 52–59.
- Wong, T. S., Brough, B., and Ho, C. M. (2009). Creation of functional micro/nano systems through top-down and bottom-up approaches. *Molecular and Cellular Biomechanics: MCB*, 6(1), 1–55.
- Wu, T., Wang, Z., Tian, M., Miao, J., Zhang, H., and Sun, J. (2018). UV excitation NO_2 gas sensor sensitized by ZnO quantum dots at room temperature. *Sensors and Actuators B: Chemical*, 259, 526–531.

- Wu, Z., Zhang, J., Benfield, R. E., Ding, Y., Grandjean, D., Zhang, Z., and Ju, X. (2002). Structure and chemical transformation in cerium oxide nanoparticles coated by surfactant cetyltrimethylammonium bromide (CTAB): an X-ray absorption spectroscopic study. *The Journal of Physical Chemistry B*, 106(18), 4569–4577.
- Xu, C., Chun, J., Rho, K., and Kim, D. E. (2005). Fabrication and photoluminescence of zinc silicate/silica modulated ZnO nanowires. *Nanotechnology*, 16(12), 2808.
- Yang, F., Cheng, S., Zhang, X., Ren, X., Li, R., Dong, H., and Hu, W. (2018). 2D organic materials for optoelectronic applications. *Advanced Materials*, 30(2), 1702415.
- Yang, R. D., Tripathy, S., Li, Y., and Sue, H. J. (2005). Photoluminescence and micro-Raman scattering in ZnO nanoparticles: The influence of acetate adsorption. *Chemical Physics Letters*, 411(1–3), 150–154.
- Yang, W., Yang, W., Kong, L., Song, A., Qin, X., and Shao, G. (2018). Phosphorus-doped 3D hierarchical porous carbon for high-performance supercapacitors: A balanced strategy for pore structure and chemical composition. *Carbon*, 127, 557–567.
- Yao, S., Swetha, P., and Zhu, Y. (2018). Nanomaterial-Enabled Wearable Sensors for Healthcare. *Advanced Healthcare Materials*, 7(1), 1–27.
- Ye, R., Jia, G., Deng, D., Hua, Y., Cui, Z., Zhao, S., Huang, L., Wang, H., Li, C. and Xu, S. (2011). Controllable synthesis and tunable colors of α -and β -Zn₂SiO₄:Mn²⁺ nanocrystals for UV and blue chip excited white LEDs. *The Journal of Physical Chemistry C*, 115(21), 10851–10858.
- Ying, Y., Ying, W., Li, Q., Meng, D., Ren, G., Yan, R., and Peng, X. (2017). Recent advances of nanomaterial-based membrane for water purification. *Applied Materials Today*, 7, 144–158.
- Yu, M., Dyer, M.J., Skidmore, G.D., Rohrs, H.W., Lu, X., Ausman, K.D., Von Ehr, J.R. and Ruoff, R.S. (1999). Three-dimensional manipulation of carbon nanotubes under a scanning electron microscope. *Nanotechnology*, 10(3), 244–252.
- Yu, X., and Wang, Y. (2009). Synthesis and VUV spectral properties of nanoscaled Zn₂SiO₄:Mn²⁺ green phosphor. *Journal of Physics and Chemistry of Solids*, 70(8), 1146–1149.
- Yun, Q., u, Q., Zhang, X., Tan, C., and Zhang, H. (2018). Three-Dimensional Architectures Constructed from Transition-Metal Dichalcogenide Nanomaterials for Electrochemical Energy Storage and Conversion. *Angewandte Chemie International Edition*, 57(3), 626–646.

- Zacharias, M., and Giustino, F. (2016). One-shot calculation of temperature-dependent optical spectra and phonon-induced band-gap renormalization. *Physical Review B*, 94(7), 075125.
- Zaid, M. H. M., Matori, K. A., Ab Aziz, S. H., Kamari, H. M., Ismail, I., Samsudin, N. F., and Rashid, S. S. A. (2017). Enhanced luminescence properties of low-cost Mn²⁺ doped willemite based glass-ceramics as potential green phosphor materials. *Journal of Materials Science: Materials in Electronics*, 28(16), 12282–12289.
- Zaid, M. H. M., Amin Matori, K., Abdul Aziz, S. H., Kamari, H. M., Mat Yunus, W. M., Abdul Wahab, Z., and Samsudin, N. F. (2016). Fabrication and crystallization of ZnO-SLS glass derived willemite glass-ceramics as a potential material for optics applications. *Journal of Spectroscopy*, 2016, 1–7.
- Zaid, M. H. M., Matori, K. A., Ab Aziz, S. H., Kamari, H. M., Wahab, Z. A., Effendy, N., and Alibe, I. M. (2016). Comprehensive study on compositional dependence of optical band gap in zinc soda lime silica glass system for optoelectronic applications. *Journal of Non-Crystalline Solids*, 449, 107–112.
- Zaid, M. H. M., Matori, K. A., Aziz, S. H. A., Kamari, H. M., Wahab, Z. A., Fen, Y. W., and Alibe, I. M. (2016). Synthesis and characterization of low cost willemite based glass-ceramic for opto-electronic applications. *Journal of Materials Science: Materials in Electronics*, 27(11), 11158–11167.
- Zaitseva, N. A., Onufrieva, T. A., Barykina, J. A., Krasnenko, T. I., Zabolotskaya, E. V., and Samigullina, R. F. (2018). Magnetic properties and oxidation states of manganese ions in doped phosphor Zn₂SiO₄:Mn. *Materials Chemistry and Physics*.
- Zdrrazil, L., Zahradnicek, R., Mohan, R., Sedlacek, P., Nejdl, L., Schmiedova, V., Pospisil, J., Horak, M., Weiter, M., Zmeskal, O. and Hubalek, J. (2018). Preparation of Graphene Quantum Dots through Liquid Phase Exfoliation Method. *Journal of Luminescence*, 204, 203–208.
- Zeng, H., Duan, G., Li, Y., Yang, S., Xu, X., and Cai, W. (2010). Blue Luminescence of ZnO nanoparticles based on non-equilibrium processes: defect origins and emission controls. *Advanced Functional Materials*, 20(4), 561–572.
- Zeng, J. H., Fu, H. L., Lou, T. J., Yu, Y., Sun, Y. H., and Li, D. Y. (2009). Precursor, base concentration and solvent behavior on the formation of zinc silicate. *Materials Research Bulletin*, 44(5), 1106–1110.
- Zhang, D. F., Sun, L. D., and Yan, C. H. (2006). Optical properties of ZnO nanoplatelets and rectangular cross-sectioned nanowires. *Chemical Physics Letters*, 422(1–3), 46–50.

- Zhang, Meili, Zhai, W., and Chang, J. (2010). Preparation and characterization of a novel willemite bioceramic. *Journal of Materials Science: Materials in Medicine*, 21(4), 1169–1173.
- Zhang, M., Wang, L., Meng, L., Wu, X.G., Tan, Q., Chen, Y., Liang, W., Jiang, F., Cai, Y. and Zhong, H. (2018). Perovskite Quantum Dots Embedded Composite Films Enhancing UV Response of Silicon Photodetectors for Broadband and Solar-Blind Light Detection. *Advanced Optical Materials*, 6(16), 1–7.
- Zhang, N., Huang, Y., and Wang, M. (2018). 3D ferromagnetic graphene nanocomposites with ZnO nanorods and Fe₃O₄ nanoparticles co-decorated for efficient electromagnetic wave absorption. *Composites Part B: Engineering*, 136, 135–142.
- Zhang, Q. Y., Pita, K., and Kam, C. H. (2003). Sol-gel derived zinc silicate phosphor films for full-color display applications. *Journal of Physics and Chemistry of Solids*, 64(2), 333–338.
- Zhang, Q. Y., Pita, K., Ye, W., and Que, W. X. (2002). Influence of annealing atmosphere and temperature on photoluminescence of Tb³⁺ or Eu³⁺-activated zinc silicate thin film phosphors via sol-gel method. *Chemical Physics Letters*, 351(3–4), 163–170.
- Zhang, S., Gao, H., Li, J., Huang, Y., Alsaedi, A., Hayat, T., Xu, X. and Wang, X. (2017). Rice husks as a sustainable silica source for hierarchical flower-like metal silicate architectures assembled into ultrathin nanosheets for adsorption and catalysis. *Journal of Hazardous Materials*, 321, 92–102.
- Zhang, X., Chen, Y., Zhang, S., and Qiu, C. (2017). High photocatalytic performance of high concentration Al-doped ZnO nanoparticles. *Separation and Purification Technology*, 172, 236–241.
- Zhang, X. P., and Cheng, X. M. (2009). Energy consumption, carbon emissions, and economic growth in China. *Ecological Economics*, 68(10), 2706–2712.
- Zhang, Z., Ye, Y., Pu, C., Deng, Y., Dai, X., Chen, X., Chen, D., Zheng, X., Gao, Y., Fang, W. and Peng, X. (2018). High-Performance, Solution-Processed, and Insulating-Layer-Free Light-Emitting Diodes Based on Colloidal Quantum Dots. *Advanced Materials*, 30(28), 1–8.
- Zhao, X., Shen, H., Zhang, Y., Li, X., Zhao, X., Tai, M., Li, J., Li, J., Li, X. and Lin, H., (2016). Aluminum-doped zinc oxide as highly stable electron collection layer for perovskite solar cells. *ACS Applied Materials and Interfaces*, 8(12), 7826–7833.
- Zhao, Y., Hong, H., Gong, Q., and Ji, L. (2013). 1D nanomaterials: synthesis, properties, and applications. *Journal of Nanomaterials*, 2013, 1.

- Zhao, Y. S., Fu, H., Peng, A., Ma, Y., Xiao, D., and Yao, J. (2008). Low-dimensional nanomaterials based on small organic molecules: Preparation and optoelectronic properties. *Advanced Materials*, 20(15), 2859–2876.
- Zhu, L., Li, Y., and Zeng, W. (2018). Hydrothermal synthesis of hierarchical flower-like ZnO nanostructure and its enhanced ethanol gas-sensing properties. *Applied Surface Science*, 427, 281–287.
- Zhu, W., Ma, X., Gou, M., Mei, D., Zhang, K., and Chen, S. (2016). 3D printing of functional biomateriengineering. *Current Opinion in Biotechnology*, 40, 103–112.

